OPTIMIZING AN *IN SITU* BIOREMEDIATION TECHNOLOGY TO MANAGE PERCHLORATE-CONTAMINATED GROUNDWATER

THESIS

Mark R. Knarr, Lieutenant, USAF

AFIT/GEE/ENV/03-14

DEPARTMENT OF THE AIR FORCE
AIR UNIVERSITY

AIR FORCE INSTITUTE OF TECHNOLOGY

Wright-Patterson Air Force Base, Ohio

The views expressed in this thesis are those of the author and do not reflect the official policy or position of the United States Air Force, Department of Defense, or the United States Government.

AFIT/GEE/ENV/03-14

OPTIMIZING AN *IN SITU* BIOREMEDIATION TECHNOLOGY TO MANAGE PERCHLORATE-CONTAMINATED GROUNDWATER

THESIS

Presented to the Faculty

Department of Systems and Engineering Management

Graduate School of Engineering and Management

Air Force Institute of Technology

Air University

Air Education and Training Command

In Partial Fulfillment of the Requirements for the

Degree of Master of Science in Engineering and Environmental Management

Mark R. Knarr, B.S.

Lieutenant, USAF

March 2003

AFIT/GEE/ENV/03-14

OPTIMIZING AN *IN SITU* BIOREMEDIATION TECHNOLOGY TO MANAGE PERCHLORATE-CONTAMINATED GROUNDWATER

Mark R. Knarr, B.S.
Lieutenant, USAF

Approved:

/signed/

Dr. Mark N. Goltz (Chairman) — March 13, 2003

/signed/

Dr. Gary Lamont (Member) — March 13, 2003

/signed/

Dr. Junqi Huang (Member) — March 13, 2003

ACKNOWLEDGMENTS

This work was supported in part by the Department of Defense Environmental Security Technology Certification Program. Furthermore, specific individuals contributed to the completion of this document, whom I will now acknowledge. First, I thank Dr. Mark Goltz for his expertise and guidance, which was probably the most helpful asset in writing my thesis. Dr. Gary Lamont provided valuable coursework and counsel on genetic algorithms, which was instrumental to this study. I owe Dr. Junqi Huang thanks for his availability and willingness to assist me with understanding the technology model. I also owe special thanks to Christopher Hendricks, an ROTC cadet at George Washington University, whose code-writing skills and patience were pivotal in putting my ideas into practice.

Mark R. Knarr

TABLE OF CONTENTS

Page

Page

Page

LIST OF FIGURES

Page

ABSTRACT

Combining horizontal flow treatment wells (HFTWs) with *in situ* biodegradation is an innovative approach with the potential to remediate perchlorate-contaminated groundwater. A technology model was recently developed that combines the groundwater flow induced by HFTWs with *in situ* biodegradation processes that result from using the HFTWs to mix electron donor into perchlorate-contaminated groundwater. A field demonstration of this approach is planned to begin this year.

In order to apply the technology in the field, project managers need to understand how contaminated site conditions and technology design parameters impact technology performance. One way to gain this understanding is to use the technology model to select engineering design parameters that optimize performance under given site conditions. In particular, a project manager desires to design a system that 1) maximizes perchlorate destruction, 2) minimizes treatment expense, and 3) attains regulatory limits on downgradient contaminant concentrations. Unfortunately, for a relatively complex technology like *in situ* bioremediation, with a number of engineering design parameters to determine, as well as multiple objectives, system optimization is not straightforward.

In this study, a multi-objective genetic algorithm (MOGA) is used to determine design parameter values (flow rate, well spacing, concentration of injected electron donor, and injection schedule) that optimize the first two objectives noted; to maximize perchlorate destruction while minimizing cost. Four optimization runs are performed, using two different remediation time spans (300 and 600 days) for two different sets of site conditions. Results from all four optimization runs indicate that the relationship

between perchlorate mass removal and operating cost is positively correlated and nonlinear. For equivalent operating times and costs, the optimized solutions show that, as expected, the technology achieves higher mass removals for the site having both higher hydraulic conductivity and higher initial source concentration. Results from all four runs show that increased perchlorate mass removal is not necessarily correlated with diminished downgradient perchlorate concentration, suggesting that it may be important to incorporate minimization of downgradient perchlorate concentration as an additional objective or constraint in the multi-objective optimization scheme.

The optimization software developed in this study can serve as a tool for both optimizing future applications of this innovative bioremediation technology, and helping us to better understand how HFTWs can be used in conjunction with *in situ* biodegradation. This study contributes to efforts taken to resolve groundwater contamination problems caused by perchlorate releases across the United States.

OPTIMIZING AN *IN SITU* BIOREMEDIATION TECHNOLOGY TO MANAGE PERCHLORATE-CONTAMINATED GROUNDWATER

1.0 INTRODUCTION

1.1 BACKGROUND

Perchlorate is an oxyanion that the aerospace industry has used since the 1940's as a constituent in solid rocket fuel (EPA, 1999:1; Herman and Frankenberger, 1998:750). Due to the absence of legal restrictions, a lack of knowledge of perchlorate health effects, and a deficient understanding of the processes affecting perchlorate fate and transport, high levels of ammonium perchlorate were discharged into the environment (Urbansky, 1998:82), resulting in perchlorate contamination problems that we face today. Perchlorate contamination from these past practices now affects the drinking water of 15 million U.S. citizens (EPA, 1999:1); this contamination is particularly significant in western states like California, Utah, and Arizona (Urbansky, 1998:82).

The chief health problem caused by perchlorate is due to its potential to interfere with hormone production in humans. The thyroid gland normally uptakes iodide from the bloodstream to make hormones; however, the presence of perchlorate in the bloodstream causes the thyroid gland to uptake perchlorate instead of iodide, thereby disrupting hormone production. Animal studies also show perchlorate's potential to

interfere with muscle movement (Urbansky, 1998:83). The presence of perchlorate in the environment triggers even more concern because the consequences of prolonged, low-dose exposure have yet to be ascertained (Logan, 2001:484A).

Unfortunately, perchlorate is mobile and persistent in the natural environment. According to Flowers and Hunt (2000:177), perchlorate is "expected to be highly mobile in surface and groundwaters". Under nearly neutral pH conditions, which are found in most groundwaters, perchlorate would probably not sorb to mineral surfaces (Flowers and Hunt, 2000:177); additionally, perchlorate ions are "not retarded during groundwater transport" (Logan, 2001:483A). Natural destruction of perchlorate is unlikely. Dissolved perchlorate salts not only resist reaction via coordination, but they also "hardly react at all in any manner"(Espenson, 2000:1). Furthermore, insufficient proof exists that perchlorate would *naturally* degrade via biological transformation (Flowers and Hunt, 2000:177).

The perchlorate problem is exacerbated because remediation of perchlorate-contaminated water is difficult. Logan (2001:484A) asserts that there is “no obvious treatment technology for removing perchlorate from water”. Ion exchange, air stripping, carbon adsorption, and advanced oxidation do not provide cost-efficient performance (Logan, 1998:70). Physical removal methods do not destroy perchlorate; they merely concentrate perchlorate elsewhere, which creates waste disposal problems (Urbansky, 1998:90). Pump-and-treat systems are poor remediation choices because they necessitate pumping contaminated water to the surface, which increases treatment costs and introduces risk of exposure to perchlorate (Ferland and Goltz, 2001:45).

In situ biodegradation, however, offers a potential solution to the perchlorate problem. According to Logan (2001:486A - 487A), injection of substrates directly into the subsurface can promote *in situ* microbial degradation; such a strategy was successful in perchlorate remediation projects at MacGregor, TX, and Sacramento, CA.

A critical issue in injecting chemicals to promote *in situ* biodegradation is ensuring the injected chemical sufficiently mixes with the contaminated groundwater. A new technology that uses so-called horizontal flow treatment wells (HFTWs) to effect mixing to promote *in situ* biodegradation has potential to remediate perchlorate contamination (McCarty *et al*., 1998; Parr, 2002). A field test at Edwards AFB, CA, successfully employed a similar technology to remediate TCE-contaminated groundwater; in that test, pulses of toluene, oxygen, and hydrogen peroxide were injected into groundwater that was circulating between two HFTWs (McCarty *et al*., 1998:88). The Environmental Security Technology Certification Program (ESTCP) funded a project to demonstrate that injection and *in situ* mixing of electron donor into perchlorate-contaminated groundwater using HFTWs could be an effective treatment technology (ESTCP, 2002). Parr (2002) developed a model that combines HFTW-induced groundwater flow with *in situ* biodegradation processes that result from use of HFTWs to mix electron donor into perchlorate-contaminated groundwater.

To apply this new technology in the field, project managers must understand how contaminated site conditions and design parameters affect technology performance. An approach to gaining this understanding is to use a technology model in order to select engineering design parameters that optimize performance for given site conditions. In particular, a project manager desires a system design that 1) maximizes perchlorate

destruction, 2) minimizes treatment expense, and 3) attains downgradient regulatory requirements.

The dilemma of pursuing separate objectives results in a multi-objective optimization problem. In multi-objective optimization, the decision maker must manipulate decision variables (*i.e.* engineering parameters) to *ideally* obtain a solution that optimizes all objectives. Furthermore, this optimum solution must be feasible (*i.e.* satisfy constraints relevant to the problem).

Unfortunately, a *single* feasible solution that optimizes all objectives usually doesn't exist. In fact, most multi-objective problems have inherent trade-off dilemmas, where improving performance in one objective usually entails worsening performance in another. For example, the decision maker may discover that reducing the operating cost of the remediation technology (desirable) incurs degraded performance in contaminant destruction (undesirable). When tradeoffs exist among competing objectives, the solution to a multi-objective problem involves finding *multiple* solutions that are nondominated, or Pareto optimal. If a solution **x** is Pareto optimal, then no other solutions exist that perform better than **x** across all objectives. Pareto optimal solutions comprise the Pareto optimal set (P*), and they exhibit a tradeoff relationship in objective space called the Pareto front (PF*) (Coello Coello *et al*., 2002:10-12).

Simultaneously optimizing performance and cost for this innovative *in situ* perchlorate bioremediation technology is a complicated undertaking; intense computational effort is necessary to handle the nonlinearities of the model's equations and account for constraints while choosing the best combination of several design variables, each of which can vary over a wide range. Hence, in order to optimize

application of the technology and gain greater understanding of technology costs and performance, it becomes necessary to select an optimization technique that can handle multiple objectives. One viable technique is the genetic algorithm (GA), a stochastic search algorithm whose operators mimic biological genetics. GAs have the ability to operate on multiple candidate solutions, as opposed to only one solution, which renders them conducive to multi-objective optimization.

1.2 RESEARCH GOALS AND OBJECTIVES

The overall goal of this thesis effort is to enhance understanding of how in situ bioremediation, used in conjunction with HFTWs, can e applied to manage perchlorate-contaminated groundwater. This goal can be divided into the following specific research objectives:

- Develop a multi-objective genetic algorithm (MOGA) that can be used in conjunction with the *in situ* perchlorate bioremediation technology model
- Determine values of design variables that optimize technology cost and performance given different time periods and contaminated-site conditions
- Assess how the technology performs in reducing downgradient concentration given different time periods and contaminated-site conditions

1.3 RESEARCH APPROACH

- Formulate a multi-objective problem (objective functions, decision variables, constraints) for application of Parr's (2002) technology model to manage perchlorate-contaminated groundwater.
- Design and encode an appropriate MOGA based on a review of the literature
- Couple the technology model with the developed MOGA
- Determine optimal technology design parameters for given site conditions

1.4 SCOPE AND LIMITATIONS OF RESEARCH

- This study assumes the technology model developed by Parr (2002) adequately simulates remediation of perchlorate-contaminated groundwater through electron donor injection by HFTWs.
- Optimization scenarios only involve a two-well HFTW system to facilitate computation. It is assumed results obtained from the two-well system can be scaled up to manage wider contaminant plumes.
- During optimization, engineering decision variables are restricted to a range of values appropriate for the formulated problem.
- MOGAs use probabilistic, rather than deterministic, operators to explore the search space for Pareto-optimal solutions. Hence, both the quantity and diversity of Pareto optimal points that a MOGA can find are inherently uncertain.
- This study limits the multi-objective problem to two objectives for the technology model: 1) mass removal of contaminant and 2) operating cost.

- This study assumes that the operating cost for the technology depends solely upon pump operation and injection of electron donor.

2.0 LITERATURE REVIEW

2.1 INTRODUCTION

This chapter begins by presenting information on perchlorate, including health effects, regulatory issues, contaminant characteristics, and remediation strategies. The next section discusses horizontal flow treatment wells (HFTWs), which may offer a means of remediating perchlorate-contaminated sites. Section 2.4 introduces the reader to multi-objective optimization, with emphasis on Pareto optimality. Section 2.5 provides an overview of genetic algorithms (GAs). Finally, Section 2.6 addresses how GAs may be applied to solve multi-objective problems.

2.2 PERCHLORATE

Perchlorate (ClO_4^-) salts are used by various industries, including the auto, chemical, rubber, and fabric industries. However, the most notable user is the aerospace industry. In the mid-1940's, the aerospace industry started large-scale production of ammonium perchlorate (NH_4ClO_4) as an oxidizer for solid rocket fuel (EPA, 1999:1). The relatively short shelf life of this chemical and absence of disposal regulations resulted in recurring discharges of ammonium perchlorate to the environment (EPA, 1999:1; Urbansky, 1998:82). More recently, demilitarization has led to missile disassembly, which may also account for discharges (Urbansky, 1998:82).

Solid salts containing perchlorate dissolve readily in water. In particular, ammonium perchlorate "is highly soluble and dissociates completely" to ammonium

(NH_4^+) and perchlorate (ClO_4^-) ions (Urbansky, 1998:82). Free perchlorate ions result in perchlorate contamination, which is now a pervasive problem in the United States. Eighteen states have confirmed contamination (Logan, 2001:483A); California, Nevada, and Arizona alone have contaminated water supplies impacting 15 million citizens (EPA, 1999:1).

Perchlorate is problematic because of its potential to interfere with hormone production in humans. Under normal circumstances, the thyroid gland extracts iodide from the bloodstream to produce hormones. Because the thyroid gland has higher selectivity for perchlorate than iodide, however, perchlorate is likely to displace iodide in the gland, thereby disrupting hormone production (Urbansky, 1998:83). The U.S. EPA (Environmental Protection Agency) observed health effects of perchlorate that was chemotherapeutically administered to patients afflicted with hyperthyroidism; after 2 months, minimum doses of 6 mg/kg/day caused "fatal bone marrow changes" (Urbansky, 1998:83). Also, animal studies show that high perchlorate concentrations can disrupt muscle movement (Urbansky, 1998:83). Uncertainty exists as to toxicity of perchlorate, particularly due to prolonged, low-dose exposure (EPA, 1999:1; Logan, 2001:484A).

Until 1997, perchlorate concentrations below 100 parts per billion (ppb) were undetectable. In April 1997, the California Department of Health Services (CDHS) developed a method to detect perchlorate levels as low as 4 ppb. Subsequent to the development of this new capability, perchlorate has been detected in the following states: AR, AZ, CA, IA, IN, KS, MD, NM, NV, NY, PA, TX, UT, and WV (EPA, 1999:1). In 1997 both California and Nevada set action levels for perchlorate at 18 ppb; in 1999 Arizona and Texas set action levels of 31 and 22 ppb, respectively (EPA, 1999:2).

Although the United States Environmental Protection Agency (USEPA) placed perchlorate on the 1998 Contaminant Candidate List, USEPA still has not issued federal drinking water regulations for perchlorate. However, on January 2, 2002, EPA did release a revised draft of its toxicity assessment for public review. The draft assessment, entitled "Perchlorate Environmental Contamination: Toxicological Review and Risk Characterization," is a culmination of research efforts since 1997 pertaining to perchlorate's health impacts (Federal Register, 2002:75-76). As of this date, however, the draft assessment is still in review.

The California Environmental Protection Agency (CEPA) proposed a public health goal (PHG) of 6 ppb perchlorate in drinking water based on a No Observed Adverse Effect Level (NOAEL) of 10 µg/kg-day and uncertainty factor of 30 (CEPA, 2002:2).

Perchlorate anions persist in the natural environment. A perchlorate anion (ClO_4^-) consists of one chlorine atom centered among four oxygen atoms in a tetrahedral structure, with the negative charge evenly distributed among the oxygen atoms (Espenson, 2000:1). This symmetric charge distribution makes the perchlorate ion resistant to complexation with metals (Espenson, 2000:1). Thus, even though perchlorate is a strong oxidant, "(p)erchlorate reactions demonstrate high kinetic barriers" that render the ion virtually unreactive and, therefore, persistent (Espenson, 2000:2). There appears to be insufficient evidence that perchlorate is biologically transformable "under natural conditions" (Flowers and Hunt, 2000:177).

In addition to persistence, perchlorate also demonstrates excellent mobility in groundwater. Reported solubility of ammonium perchlorate is relatively high at 200 g/L,

and “sodium, calcium, and magnesium salts are even more soluble” (Flowers and Hunt, 2000:177). Under nearly neutral pH conditions typical of most groundwater, sorption of perchlorate to mineral surfaces is unlikely (Flowers and Hunt, 2000:177) and perchlorate ions are "not retarded during groundwater transport" (Logan, 2001:483A).

Methods to treat perchlorate-contaminated groundwater can be implemented in two ways: *ex situ* (above ground) or *in situ* (in place, below ground). *Ex situ* treatment necessitates application of a pump-and-treat (PAT) system to pump the contaminated water from the subsurface to the surface where treatment occurs. Disadvantages of PAT are discussed in Section 2.3. However, *ex situ* treatment is advantageous because it allows implementation of various conventional and innovative treatment methods, such as anion exchange, reverse osmosis (RO), chemical/electrochemical reduction, and engineered biotreatment. A more detailed discussion of each of these methods follows.

Anion exchange is an existing technology that uses a resin to extract aqueous perchlorate and replace it with an innocuous anion (Urbansky and Schock, 1999:86). Unfortunately, current resins have poor selectivity for perchlorate, and resins with enhanced selectivity are expensive (Urbansky and Schock, 1999:84). Selectivity for perchlorate worsens at lower perchlorate concentrations because resins tend to favor more abundant anions for exchange (Urbansky and Schock, 1999:84). Resins can remove aqueous perchlorate only until an equilibrium concentration occurs, after which further removal is impossible (Urbansky and Schock, 1999:84). Time is lost regenerating the resin (Urbansky and Schock, 1999:84), and brines used to regenerate resins can have perchlorate concentrations high enough to warrant disposal concerns (Logan, 2001:484A).

In RO, high pressure forces untreated water through a semiporous polymer membrane (Urbansky and Schock, 1999:86). The membrane, which is impermeable to dissolved salts, acts as a filter (Urbansky and Schock, 1999:86). Water passes through the membrane and dissolved salts stay behind, so that the membrane-filtered water is relatively deionized (Urbansky and Schock, 1999:87). However, RO membranes are susceptible to fouling from metallic compounds, natural organic matter, and microbes; such fouling necessitates costly membrane replacement (Urbansky, 1998:89; Urbansky and Schock, 1999:86-87).

Because anion exchange and RO are both physical removal methods, they have a common drawback: waste disposal (Urbansky and Schock, 1999:85; Urbansky, 1998:90). Physical removal merely transfers perchlorate from water to another medium instead of destroying it. The transferred perchlorate must either undergo further treatment or disposal. As Urbansky (1998) says, "Although these techniques take the perchlorate out, they concentrate it somewhere else where it must be dealt with later" (90).

Ex situ perchlorate destruction is possible with innovative technologies, such as electrochemical reduction, reduction using titanous ions or metallic iron/UV light, and biological treatment. In electrochemical reduction, a cathode applies electric current directly to water at a high potential to reduce perchlorate to chloride (Urbansky and Schock, 1999:85). However, movement of perchlorate ions toward the electrode can take a long time, and electrodes are susceptible to corrosion and fouling from natural organic matter (Urbansky and Schock, 1999:85).

Earley *et al*. (2000) hypothesized that perchlorate might be effectively destroyed by reaction with trivalent titanous ions [$Ti(H_2O)_6^{3+}$] in an ethanol media, which catalyze

the reaction. Amadei and Earley (2001) also proposed catalysts that offer faster reaction rates than ethanol media. Parr (2002) points out, however, that this technology has "very limited laboratory data," and pilot-scale tests have yet to be accomplished (63).

According to Gurol and Kim (2000), exposing perchlorate to UV light and metallic iron (Fe^0) under anoxic conditions can transform perchlorate to chloride and water. It is hypothesized that metallic iron first adsorbs the perchlorate ion and then undergoes oxidation, with UV light expediting the electron transfer from the iron to the perchlorate. However, high reaction rates were achievable only with very high UV intensity (Gurol and Kim, 2000). Limited data on the metallic iron/UV technology suggest this technology is currently inappropriate for lowering perchlorate levels to below regulatory limits (Parr, 2002:63).

Research on *ex situ* engineered biological treatment ("biotreatment") of perchlorate-contaminated water has largely focused on flowing water through a column-type bioreactor to effect treatment. In general, these bioreactors contain microbial support media (GAC, sand, plastic) that are inoculated with perchlorate-reducing microbes (PRMs). Inflow is a mixture of perchlorate and substrate (electron donor). Inside the reactor, PRMs reduce perchlorate via the following pathway (Rikken *et al*., 1996:425):

ClO_4^- (perchlorate) $\rightarrow$ ClO_3^- (chlorate) $\rightarrow$ ClO_2^- (chlorite) $\rightarrow$ Cl^- (chloride) + O_2

In this sequential reduction, the substrate acts as an electron donor, and perchlorate acts as the terminal electron acceptor.

The two primary designs of *ex situ* bioreactors are fluidized- and fixed-bed. Fluidized-bed reactors use high flow rates to mix the support medium (GAC, sand)

within the reactor (Logan, 2001:485A). In fixed-bed reactors, the support medium remains stationary ("fixed") during water treatment (Logan, 2001:485A). Pilot versions of fluidized- and fixed-bed bioreactors have demonstrated the ability to reduce perchlorate concentrations to below the current detection limit (4 ppb). Full-scale fluidized-bed reactors in California have effectively reduced perchlorate levels to < 4 ppb as well (Hatzinger *et al*., 2000:7; Greene and Pitre, 2000:252).

In situ methods offer the ability to treat perchlorate-contaminated water while it is still in the ground. *In situ* methods are favorable because, unlike *ex situ* methods, they do not require pumping groundwater to the surface for treatment, thereby reducing both operating expenses and human exposure to the contaminant. However, *in situ* treatment technologies are limited to those technologies that can be applied in-well or below ground. Parr (2002) surveyed perchlorate treatment technologies and determined that biotreatment is the only method readily applicable for *in situ* use.

Both *in situ* and *ex situ* biotreatment rely on the same reaction pathway (Rikken *et al*., 1996:425) to desynthesize perchlorate. However, *in situ* biotreatment requires 1) presence of PRMs at the contaminated site and 2) a means of creating anoxic conditions for perchlorate reduction (Logan, 2001:486A). The first requirement is perhaps the easiest to fulfill. PRMs appear to be found in soil at perchlorate-contaminated sites and are "widely distributed in nature" (Wu *et al*., 2001:119, 125). To fulfill the second requirement, Logan (2001) proposes either use of biobarriers or direct injection of substrates into the ground (486A-487A).

Biobarriers may be a cost-effective way of implementing *in situ* biotreatment (McMaster *et al*., 2001:301). A biobarrier contains "high concentrations of organic

matter" and establishes a vertical zone of bioactivity in the ground (Logan, 2001:486A-487A; Domenico and Schwarz, 1998:450). As contaminated groundwater passes through the barrier, microorganisms chemically transform the target contaminant (Domenico and Schwarz, 1998:450). A biobarrier is a "passive" remediation technology that can remain in-ground for years with negligible maintenance (Domenico and Schwarz, 1998:450). In MacGregor, TX, biobarriers were used to remediate soil contaminated with high levels of perchlorate (Logan, 2001:487A). Biobarriers were installed by digging trenches and filling them with organic materials and gravel (Logan, 2001:487A). By directing water flow through the biobarrier, perchlorate dropped from 27,000 µg/L to nondetectable levels (Logan, 2001:487A). As a passive technology, however, biobarriers may be bypassed as groundwater flow conditions change over time. In addition, biobarriers can only be emplaced to a limited depth.

Injection of substrates into the ground is another *in situ* biotreatment strategy (Logan, 2001:486A-487A). In May 2000 a field demonstration at the Aerojet Superfund Site in Sacramento, CA, showed the effectiveness of *in situ* biodegradation of perchlorate (McMaster *et al*., 2001:297). The test site had a perchlorate plume with concentrations ranging from 10,000 – 15,000 µg/L. A closed-loop recirculation system, located within the plume's center, extracted water from the aquifer, added time-pulsed doses of acetate, and injected the mixture back into the aquifer to stimulate bioactivity. The system reduced perchlorate levels to <18 µg/L, the CDHS action level for perchlorate in drinking water (McMaster *et al*., 2001:297, 299). Note however, that the closed-loop recirculation system applied at the Aerojet Site required extraction and reinjection of groundwater, using a strategy similar to PAT. In order to effectively achieve injection and mixing of

substrate into perchlorate-contaminated groundwater, and delivery of the mixture to indigenous PRMs, without the need to pump water to the surface, an innovative technology has been proposed (Parr, 2002). This technology, horizontal flow treatment wells (HFTWs), is discussed in the next section.

2.3 HORIZONTAL FLOW TREATMENT WELL (HFTW) SYSTEM

The operating concept for an HFTW system is for the treatment wells to be installed at the distal end of a contaminant plume. The plume would be captured by the wells and the contaminated groundwater treated (*i.e.* contaminant mass destroyed) so that contaminant concentrations downgradient of the treatment wells would meet regulatory requirements (Ferland and Goltz, 2001:46). Figures 1 and 2 show cross-sectional and plan views, respectively, of HFTW operation.

As shown in Figure 1, an HFTW has two screens, each located in a different subsurface horizon. The HFTW extracts contaminated groundwater through a screen in one horizon, treats the water, and then discharges the water through the screen in the other horizon. In-well treatment can involve the application of a physical, chemical, or biological process to remove or destroy the contaminant (Gandhi *et al*., 2002a:4); or, as depicted in the figure, it can involve injection of chemicals into the flowing contaminated groundwater in order to establish bioactive zones outside the wells' discharge screens, where the contaminant is biodegraded by indigenous microorganisms (McCarty *et al*., 1998:90). HFTWs are installed in pairs, with one well pumping in an "upflow mode" while the adjacent well pumps in a "downflow mode," resulting in water recirculating

between the two wells in a horizontal flow pattern (Ferland and Goltz, 2001:46). This is in contrast to the flow pattern induced by the better-known groundwater circulation wells (GCWs) where water circulates vertically between the two well screens of a single GCW (Parsons, 2002).

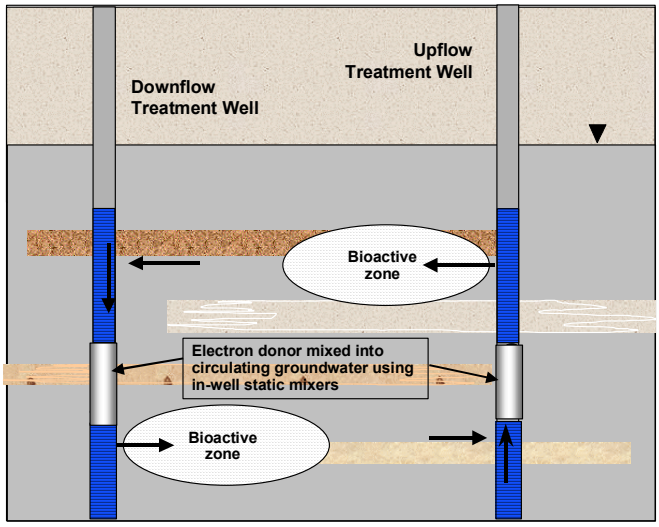

Figure 1. Cross-sectional view of HFTW operation.

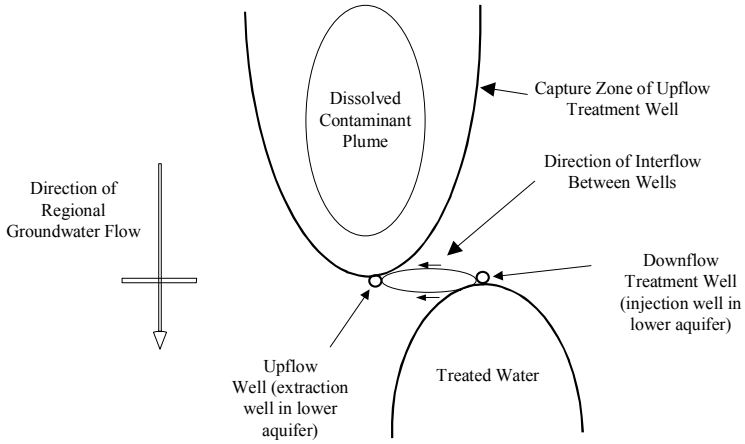

Figure 2. Plan view of HFTW operation.

HFTWs offer several advantages over conventional treatment technologies like pump-and-treat (PAT) and permeable reactive barriers (PRBs). Unlike PAT systems, HFTWs do not pump contaminated groundwater to the surface. Eliminating the need to

extract groundwater is economically advantageous because it eliminates the expense of (1) pumping groundwater to the surface and (2) disposing of the contaminant (McCarty *et al*., 1998:99). Also, treating the contaminated water in the subsurface reduces risk of exposure to the contaminant (Gandhi *et al*., 2002a:4-5). Another advantage of HFTWs when compared to PAT systems is that after a PAT system withdraws water from a contaminated zone, the hydraulic gradient that was established by the capture well continues to draw freshwater into that same zone; "contaminants sorbed to the soil in that zone desorb and contaminate this freshwater" (McCarty *et al*., 1998:99). Hence, pristine groundwater becomes contaminated and unusable. This is especially problematic in water shortage areas, especially if regulations prohibit returning treated water to the ground. HFTWs are superior to PAT systems in this regard because the treatment wells inject water immediately after extracting it, so pristine groundwater is not drawn into the contamination zone (McCarty *et al*., 1998:99).

Recirculation between HFTWs results in water with dissolved contaminants passing multiple times through the treatment zones, which as noted earlier may either be in-well or bioactive zones external to the well. This recirculation results in higher contaminant destruction efficiencies than are possible with single-pass systems, such as PRBs (Ferland and Goltz, 2001:46; Gandhi *et al*., 2002:4-5). Although PRBs, like HFTWs, is an *in situ* treatment technology (Domenico and Schwarz, 1998:450), the fact that PRBs are passive results in significant disadvantages. For one thing, PRBs may only be applied under certain conditions (for instance, where the contamination plume is relatively shallow, so that a barrier that can intercept the entire depth of the plume can be economically emplaced). In addition, changing flow conditions can allow a

contamination plume to bypass the PRB or result in insufficient residence time within the reactive barrier to adequately treat the contaminant. An HFTW, on the other hand, is an active technology that captures contaminated water by pumping. Control of flow and recirculation also assures treatment efficiency is adequate.

The effectiveness of HFTWs was demonstrated at a field test at Site 19, Edwards AFB, CA. This field test employed HFTWs to remediate two aquifers, an upper water table aquifer and a lower confined aquifer, each contaminated with 500-1200 μg/L TCE. The test involved pulsed injections of toluene, oxygen, and hydrogen peroxide into a pair of HFTWs. The two treatment wells were spaced 10 m apart, and each well pumped contaminated water at a rate of 38 L/min (McCarty *et al*., 1998:88).

Each treatment well had two screens (one in the upper aquifer and the other in the lower aquifer) for groundwater to enter/exit the well. One treatment well extracted groundwater from the *upper* aquifer, used an in-well mixer to add toluene, oxygen, and hydrogen peroxide into the contaminated water, and discharged the water into the *lower* aquifer. Conversely, the second treatment well extracted groundwater from the *lower* aquifer, mixed the additives into the contaminated water, and discharged the water into the *upper* aquifer. This strategy resulted in development of (1) *in situ* zones of bioactivity near the discharge screens of the two treatment wells, where toluene was aerobically oxidized, and TCE cometabolized, and (2) groundwater circulation cells between the two treatment wells (McCarty *et al*., 1998:90). It was demonstrated that HFTW operation resulted in: (1) efficient mixing of amendments into contaminated groundwater without the need to pump the groundwater to the surface, and (2)

recirculation between the treatment wells, resulting in multiple passes of contaminated water through the bioactive zones, where treatment was effected.

Regional groundwater upgradient of the HFTW system had dissolved TCE concentrations of about 1000 μg/L; downgradient of the system, groundwater had much lower concentrations of 18 – 24 μg/L, indicating 97 – 98% overall removal efficiency (McCarty *et al*., 1998:99). Thanks to recirculation between the two treatment wells, it was possible to attain these high removals even though only 87% contaminant destruction was achieved with each single pass of contaminated groundwater through the bioactive zones that were established around the injection screens of the treatment wells (McCarty *et al*., 1998:88).

Christ *et al.* (1999) developed an analytical model to investigate application of multiple injection and extraction well pairs to remediate groundwater contaminated with TCE. Overall efficiency (η) of an HFTW system, which is a measure that compares contaminant concentrations upgradient and downgradient of the system, is a function of the single-pass contaminant removal efficiency and interflow of water between the treatment wells (Christ *et al*., 1999:297, 298). Christ *et al*. (1999) defines single-pass contaminant removal efficiency, η_{sp}, as "contaminant removal for each pass of water through the treatment zone" (297). For the two-well HFTW system shown in Figure 1, there would be two single-pass contaminant removal efficiencies, η_{spU} and η_{spL}, for the treatment zones in the upper and lower horizons, respectively (Christ, 1997:p3-27).

To understand the definition of interflow, let us assume we are dealing with a two-well injection/extraction system. In this simple system, interflow is defined as the water flowing into the extraction well that originated in the injection well, normalized by

the total flow in the extraction well (Christ *et al*., 1999:298). For a multi-well system, with all wells pumping at the same rate, total interflow is defined as the flow through all the extraction wells that originated in injection wells, normalized by the flow through a single extraction well. We may also define a parameter that we will call average interflow (I_{avg}) as the total interflow divided by the number of extraction wells. Note for the two-well system we described above, total interflow equals average interflow.

Interflow is a function of system design parameters such as pump rate and well spacing, as well as environmental conditions such as groundwater regional flow and aquifer thickness. The reader may refer to Christ *et al*. (1999) for details on how to analytically calculate average interflow for given engineered and environmental parameters, under various simplifying conditions (homogeneity, horizontal steady flow, etc.).

By definition, overall treatment efficiency is:

$$\eta = 1 - C_{out}/C_{in} \qquad (2.1)$$

where C_{in} and C_{out} are contaminant concentrations upgradient and downgradient of the treatment system, respectively (Christ *et al*., 1999:304). By mass balance, overall treatment efficiency can also be expressed as

$$\eta = \frac{\eta_{sp}}{1 - I_{avg}(1 - \eta_{sp})} \qquad (2.2)$$

If we assume that the contaminant concentration, C_{in}, upgradient of a two-well HFTW system is equal for both upper and lower treatment horizons, we may derive expressions for concentrations downgradient of the system for both the upper (C_{outU}) and lower (C_{outL}) treatment horizons. If we also assume there is no interflow between the

injection and extraction screens of a single treatment well, the following equations for (C_{outU}) and lower (C_{outL}) apply (Christ, 1997:p3-27).

$$C_{outU} = C_{in}\left(\frac{(1-I_L)(1-\eta_{spU}) + I_L(1-I_U)(1-\eta_{spL})(1-\eta_{spU})}{1-I_U I_L(1-\eta_{spL})(1-\eta_{spU})}\right) \qquad (2.3)$$

$$C_{outL} = C_{in}\left(\frac{(1-I_U)(1-\eta_{spL}) + I_U(1-I_L)(1-\eta_{spL})(1-\eta_{spU})}{1-I_U I_L(1-\eta_{spL})(1-\eta_{spU})}\right) \qquad (2.4)$$

where

C_{in} = upgradient concentration, upper and lower horizons
C_{outU} = downgradient concentration, upper horizon
C_{outL} = downgradient concentration, lower horizon
I_U = interflow, upper horizon
I_L = interflow, lower horizon
η_{spU} = single-pass contaminant removal efficiency, upper horizon
η_{spL} = single-pass contaminant removal efficiency, lower horizon

Ferland combined Christ's (1997) analytical model of groundwater flow induced by HFTWs with a submodel simulating dehalogenation of chlorinated ethenes using a metal catalyst (Ferland, 2000; Ferland and Goltz, 2001). The submodel simulated first-order destruction of chlorinated ethenes in in-well reactors containing palladium-based catalysts. Stoppel extended Ferland's (2000) model to account for catalyst deactivation and regeneration (Stoppel, 2001; Stoppel and Goltz, 2002).

The disadvantage to modeling HFTWs using an analytical solution is the requirement that many simplifying assumptions such as homogeneity and strictly horizontal flow must be made. Numerical modeling, on the other hand, allows for a more accurate simulation of real conditions, as a numerical model can accommodate heterogeneity and anisotropy. Under these more realistic and complex conditions, a

numerical flow model like MODFLOW (Harbaugh and McDonald, 1996) can be used to determine interflow.

Both Huang and Goltz (1998) and Gandhi *et al.*, (2002) developed numerical flow-and-transport models to simulate TCE biodegradation in an HFTW system. The 3-dimensional Huang and Goltz (1998) model accounts for multi-dimensional flow, advective/dispersive transport of dissolved species, equilibrium or rate-limited sorption, and biodegradation (281). A partial-implicit approach is used to numerically solve a set of nonlinear partial differential equations describing fate and transport of TCE, toluene, oxygen, and microbes (Huang and Goltz, 1998:281).

Gandhi *et al.* (2002a) developed a 3-dimensional, numerical model to simulate the HFTW system used at Site 19, Edwards AFB, which was previously discussed. Gandhi *et al.* (2002a) used a finite-element approach in order to 1) enhance flexibility in locating both monitoring and treatment wells and to 2) provide smaller grid dimensions where high spatial resolution is critical (i.e., near pumping wells) (Gandhi *et al.*, 2002a:10). The 3-dimensional model accounted for advective-dispersive transport, biodegradation, and inhibition of biomass growth due to hydrogen peroxide, which was used as a source of oxygen (Gandhi *et al.*, 2002b:2). Model simulations and field data of TCE and dissolved oxygen concentrations were reasonably consistent (Gandhi *et al.*, 2002b:26). Gandhi *et al.* (2002b) points out that, despite the heterogeneity that's inherent in any aquifer, the model adequately simulated operation of the HFTW system even when a homogeneous hydraulic conductivity field was assumed (26). It appears that the flow field imposed by operation of the HFTW system results in reduction of the effects of heterogeneity on treatment system performance (Gandhi *et al.*, 2002b:26).

For this thesis, the system of interest involves HFTWs to remediate a perchlorate-contaminated site. The author intends to optimize multiple objectives for this system, so the next section introduces multiple-objective optimization.

2.4 MULTIPLE OBJECTIVE OPTIMIZATION

A multi-objective optimization problem (MOP) consists of decision variables, two or more objective functions, and constraints. These three components of an MOP are defined as follows:

- decision variables: variables whose numerical values are controlled by the decision maker.
- objective function: a function that maps decision variable values to values reflecting a performance level; optimizing this performance level entails either maximization or minimization.
- constraints: restrictions imposed by the particular problem that must be satisfied to render a solution acceptable. "They describe dependences among decision variables and constants (or parameters) involved in the problem" (Coello Coello *et al*., 2002:5). If solutions satisfy all constraints, then they are feasible; otherwise, they are infeasible.

For example, suppose a site engineer wishes to install a 2-well pump-and-treat (PAT) system at a site contaminated with TCE. The engineer has control over the location and pump rate of each well. The engineer wishes to simultaneously maximize contaminant mass removal and minimize operating costs. The contaminated site is

rectangular, measuring 200 meters east-west and 300 meters north-south. To prevent excessive drawdown, the pump rate of each well must be ≤ 200 m^3/day.

In this example, there are 6 decision variables: the east-west location of each well (a_1, a_2), the north-south location of each well (b_1, b_2), and the pump rate of each well (Q_1, Q_2). These decision variables can be represented by a single decision variable vector, $\mathbf{x}$ = [a_1, a_2, b_1, b_2, Q_1, Q_2]. The objective functions can be represented by the vector $\mathbf{f}(\mathbf{x})$ = [$f_1(\mathbf{x})$, $f_2(\mathbf{x})$], where $f_1(\mathbf{x})$ = mass TCE removed, and $f_2(\mathbf{x})$ = treatment cost. The constraints of the problem are as follows:

$$0 \le a_i \le 200 \text{ meters, for } i = 1, 2$$

$$0 \le b_i \le 300 \text{ meters, for } i = 1, 2$$

$$0 \le Q_i \le 200 \text{ } m^3/\text{day, for } i = 1, 2$$

Now consider a more general formulation of a multiobjective problem. Consider a decision variable vector $\mathbf{x}$ = [x_1, $x_2 \ldots x_n$] in which elements x_1, $x_2 \ldots x_n$ are decision variables. Also consider an objective function vector $\mathbf{f}(\mathbf{x})$ = [$f_1(\mathbf{x})$, $f_2(\mathbf{x}) \ldots f_k(\mathbf{x})$] in which elements $f_1(\mathbf{x})$, $f_2(\mathbf{x}) \ldots f_k(\mathbf{x})$ are objective functions to be maximized or minimized. Also consider a constraint function vector $g(\mathbf{x})$ = [$g_1(\mathbf{x})$, $g_2(\mathbf{x}) \ldots g_m(\mathbf{x})$] in which each element is a constraint of the form $g_i(\mathbf{x}) \le 0$ for i = 1, 2…m. Then an MOP is formally defined as the search for the optimum solution vector $\mathbf{x}^*$ = [x^*_1, $x^*_2 \ldots x^*_n$] that optimizes $\mathbf{f}(\mathbf{x})$ = [$f_1(\mathbf{x})$, $f_2(\mathbf{x}) \ldots f_k(\mathbf{x})$] and satisfies the constraint vector $g(\mathbf{x})$ = [$g_1(\mathbf{x})$, $g_2(\mathbf{x}) \ldots g_m(\mathbf{x})$]. The constraint vector $g(\mathbf{x})$ establishes the **feasible region** Ω, and any solution vector $\mathbf{x} \in \Omega$ is defined as a **feasible solution** (Coello Coello *et al*., 2002:7).

Unfortunately, practical MOPs do not have a single solution $\mathbf{x}^* \in \Omega$ that optimizes *all* objective functions. Under normal circumstances, improving performance in one objective mandates worsening performance in another; a "trade-off" dilemma occurs among objectives that conflict with each other. Inability to universally optimize all elements of $\mathbf{f}(\mathbf{x})$ renders the word "optimum" controversial in the MOP arena. Therefore, determining the optimum solution ultimately rests with the preferences of the decision maker, making the determination subjective rather than objective (Sawaragi *et al*., 1985:25; Ringuest, 1992:2).

Despite this subjectivity, the concept of **dominance** enables the decision maker to objectively distinguish superior solutions from inferior ones. Dominance is mathematically definable. Suppose all objective functions of $\mathbf{f}(\mathbf{x}) = [f_1(\mathbf{x}), f_2(\mathbf{x}) \ldots f_k(\mathbf{x})]$ are to be minimized (this supposition is legitimate because any maximization function can be expressed as a minimization function by simply multiplying the function by -1), and two vectors ($\mathbf{x}_1$ and $\mathbf{x}_2 \in \Omega$) exist. Then, for i = 1, 2…k, $\mathbf{x}_2$ **dominates** $\mathbf{x}_1$ if and only if the following condition is true (Coello Coello *et al*., 2002:11):

$$\forall\ i,\ f_i(\mathbf{x}_2) \leq f_i(\mathbf{x}_1) \text{ and } \exists\ i \mid f_i(\mathbf{x}_2) < f_i(\mathbf{x}_1) \qquad (2.5)$$

The first condition means that $\mathbf{x}_2$ performs the *same or better than* $\mathbf{x}_1$ with respect to *all* objective functions; the second condition means that $\mathbf{x}_2$ performs *better* than $\mathbf{x}_1$ with respect to *at least one* objective function.

Furthermore, if there is no $\mathbf{x} \in \Omega$ that dominates $\mathbf{x}_2$, then $\mathbf{x}_2$ is called **nondominated**, or **Pareto-optimal**. Still assuming all $f_i(\mathbf{x})$ are to be minimized, the vector $\mathbf{x}^*$ is Pareto-optimal if, for every $\mathbf{x} \in \Omega$ and i = 1, 2…k, either of the following conditions is true (Coello Coello *et al*., 2002:10):

$$\exists\, i \mid f_i(\mathbf{x}^*) < f_i(\mathbf{x}) \quad \text{or} \quad \forall\, i,\ f_i(\mathbf{x}^*) = f_i(\mathbf{x}) \qquad (2.6)$$

Nondomination, or Pareto-optimality, is an essential property of any candidate solution to an MOP (Ringuest, 1992:3). The set of all Pareto-optimal solutions to an MOP is called the **Pareto-optimal set**, which is defined as

$$P^* := \{\mathbf{x} \in \Omega \mid \neg\exists\ \mathbf{x}' \in \Omega,\ \forall\, i,\ f_i(\mathbf{x}) \le f_i(\mathbf{x}') \text{ and } \exists\, i\ f_i(\mathbf{x}) < f_i(\mathbf{x}')\} \qquad (2.7)$$

In other words, each element of P* is a decision variable vector **x** that is both feasible and Pareto-optimal. Coello Coello (2002) emphasizes that a solution's membership in P* depends on its evaluation with *all* objective functions (12-13). The mapping of all solutions in P* to their objective function values is called the **Pareto front** (PF*). The Pareto front is defined as follows (Coello Coello *et al*., 2002:12):

$$PF^* := \{\mathbf{f}(\mathbf{x}) = [f_1(\mathbf{x}), f_2(\mathbf{x}) \ldots f_k(\mathbf{x})] \mid \mathbf{x} \in P^*\} \qquad (2.8)$$

The reader should understand that P* pertains to *decision variable* values whereas PF* pertains to the *objective function* values. The symbolic relationship between P* and PF* can be written as

$$P^* \xrightarrow{\text{objective functions}} PF^* \qquad (2.9)$$

Each member $\mathbf{x} \in P^*$ is a particular array of *decision variable* values. Each member $\mathbf{f}(\mathbf{x}) \in PF^*$ is a particular combination of *objective function* values corresponding to $\mathbf{x} \in P^*$.

P* represents the *true* Pareto-optimal set. In other words, P* is an exhaustive set of nondominated solutions (possibly infinite). In the real world, however, generating P* is not viable for several reasons. First, generating an infinite number of solutions is impossible, so the solutions that are generated are only a subset of P*. Second, computational precision limits may render solutions that are not identical to the *truly*

Pareto optimal solutions. For these reasons, a set of real-world MOP solutions is just a discontinuous approximation of P*, and this approximation is denoted P_{known}.

The distinction between "true" and "approximate" also applies to the Pareto front. For complex MOPs, deriving an analytical expression for the *true* Pareto front PF* is usually impossible (Coello Coello, 2002:12; Veldhuizen and Lamont, 2000:128); an alternative method for generating PF* involves mapping each $\mathbf{x} \in P^*$ to its objective function value (Coello Coello, 2002:12). As stated previously, however, computational limitations only permit us to generate P_{known} instead of P*; so mapping P_{known} to objective function space yields PF_{known}, which approximates PF*. The relationship between P_{known} and PF_{known} is analogous to the relation ship between P* and PF* and can be represented symbolically:

$$P_{known} \xrightarrow{\text{objective functions}} PF_{known} \qquad (2.10)$$

Given this discussion, the following procedure is typical for solving real-world MOPs:

- Generate P_{known} as an estimate of P*
- Generate PF_{known} by evaluating the objective function vector for each $\mathbf{x} \in P_{known}$
- Choose a solution from P_{known} that results in an acceptable value of the corresponding PF_{known} on the Pareto front. "Acceptable" is a subjective term, dependent upon the decision maker's preferences.

A popular stochastic search algorithm, known as the genetic algorithm (GA), is well-adapted to solving complex MOPs. More about GAs follows in the next section.

2.5 GENETIC ALGORITHMS

John H. Holland (1975) from the University of Michigan pioneered the stochastic search technique known as the genetic algorithm (GA). A genetic algorithm searches for solutions using principles analogous to evolution and biological genetics. According to Whitley (1994), a GA is "any population-based model that uses selection and recombination operators to generate new sample points in a search space." Goldberg (1989) distinguishes the genetic algorithm from traditional search methods, like calculus-based, enumerative, and random search methods in four ways:

1. GA requires that the user encode the problem's parameters as a data structure ("string"). Mitchell (1996) points out that this step is crucial for a GA to be successful (156).
2. GA operates on a population of candidate solutions – not just one solution.
3. GA neglects auxiliary and derivative information; the only information that is crucial are objective function values associated with the strings.
4. GA uses probabilistic transition rules to explore the search space instead of deterministic rules.

The terminology associated with genetic algorithms borrows heavily from biology. Some common terms are defined here:

Chromosome: an encoded string representing a complete parameter set or solution to a problem; often used interchangeably with "string"

Gene: a subunit of a chromosome dedicated to a particular parameter

Allele: specific value that a gene may assume

Genotype: the specific content of a chromosome that distinguishes one chromosome from another

Phenotype: the decoded version of a chromosome; value(s) obtained by evaluating a chromosome with its objective function(s)

Fitness: a measure of how "good" a chromosome is, which is related to its evaluation (phenotype); a fitness function converts a chromosome's evaluation "into an allocation of reproductive opportunities" (Whitley, 1994),

Using the example of the PAT system from Section 2.4 (multi-objective problems), each decision variable (a_1, a_2, b_1, b_2, Q_1, Q_2) would be a *gene*; the aggregation of these variables is the vector **x**, which a GA would treat as a *chromosome*. Using the same convention from section 2.4, consider two hypothetical vectors (chromosomes) $\mathbf{x}_1$ and $\mathbf{x}_2$ such that

$$\mathbf{x}_1 = [156, 187, 275, 24, 150, 180] \text{ and } \mathbf{x}_2 = [32, 114, 101, 299, 100, 200]$$

Vectors $\mathbf{x}_1$ and $\mathbf{x}_2$ consist of the same decision variables (*genes*), but they assume different values (*alleles*). Because corresponding alleles of $\mathbf{x}_1$ and $\mathbf{x}_2$ are dissimilar, they have different *genotypes*. Suppose TCE mass removal is the only objective function f(**x**), and $f(\mathbf{x}_1) = 5.2$ kg, and $f(\mathbf{x}_2) = 8.7$ kg. The values 5.2 kg and 8.7 kg are the *phenotypes* of $\mathbf{x}_1$ and $\mathbf{x}_2$, respectively. If mass removal is the only metric for chromosome performance, then chromosome $\mathbf{x}_2$ has better *fitness* than $\mathbf{x}_1$.

Goldberg (1989) identifies three fundamental GA operators: reproduction, crossover, and mutation (10). **Reproduction** (or **selection**) means that the GA reproduces/selects chromosomes from the initial population and places them into a temporary mating pool. Usually, the GA is constructed so that the probability a particular chromosome is

reproduced is proportional to that chromosome's fitness. Hence, chromosomes with higher fitness have higher probability of reproduction; lower-fitness chromosomes have less probability. This is analogous to Charles Darwin's notion of "survival of the fittest."

After reproduction, the mating pool is filled and the chromosomes are ready to undergo **crossover**. In crossover, the GA probabilistically "mates" chromosomes at random, causing them to exchange portions of themselves with each other. The crossover operator hopefully combines desirable characteristics of those higher-fitness chromosomes to make even better chromosomes. Crossover probability usually ranges from 0.4 to 0.9 (Coley, 72:1999). Finally, **mutation** may occur. The GA, by some small probability, mutates a chromosome by changing one or more alleles. Because mutation probability tends to be orders of magnitude less than crossover probability (14), mutation has less influence on chromosomes than crossover. After mutation, the new population of chromosomes is complete. Each cycle of fitness evaluation, reproduction, crossover, and mutation is called a **generation**.

The following pseudo code represents a very simple GA:

Initialize population of strings/chromosomes

Repeat until desired number of generations is attained

Evaluate fitness (objective function) for each string

Reproduce strings to mating pool based on fitness

Perform cross-over

Mutate alleles

End

Reproduction, crossover, and mutation address the trade-off dilemma between exploitation and exploration that plagues any search algorithm. *Exploitation* is the strategy of using knowledge of previous points in the search space to locate even better points; e*xploration*, on the other hand, is the investigation of new and unknown areas of the search space (Beasley *et al*, 1993:63). Efforts to exploit diminish efforts to explore, and vice versa. Although exploitation is useful because it focuses on a promising area of the search space, excessive exploitation causes the algorithm to neglect other areas of search space that may contain better solutions. Conversely, exploration gives the algorithm freedom to "travel" the search space, but too much exploration has the danger of degenerating into a haphazard random search.

The reproduction and crossover operators are the exploiting power of the GA; they work cooperatively to improve successive generations of chromosomes. However, a problem arises if these two operators work strictly by themselves: continuously disregarding lower-fitness chromosomes directs the search to a very concentrated portion of the search space and diminishes the potential to find better chromosomes elsewhere. This is why the GA uses mutation to provide some exploring power. As Beasley *et al* (1993) states, "mutation provides a small amount of random search, and helps ensure that no point in the search space has a zero probability of being examined" (60).

The reason GAs work is because of the Fundamental Theorem of Genetic Algorithms, better known as the Schema Theorem. A **schema** (plural **schemata**) is a template describing a subset of strings with similar allele patterns (Holland, 1992:68; Goldberg, 1989:19). It is a chromosome template that consists of alleles plus a "wildcard" symbol (*) that can assume any allele.

Consider a chromosome population whose individual genes are represented with the binary alphabet (0, 1). The schema [**11**0*] has length = 6 and contains fixed alleles in the first, second, and fifth position; the remaining alleles are *'s that can assume values of 0 or 1. The schema [**11**0*] can represent the following strings: [**11**01**0**1], [**11**10**0**0], and [**11**00**0**1].

Two important characteristics of a particular schema is its order and defining length. **Order** is the number of fixed alleles (i.e. all alleles except *), and **defining length** is the distance between the first and last *fixed* alleles (Michalewicz, 1996:46). The example schema [**11**0*] has order = 3 because positions 1, 2, and 5 are fixed. Schema [**11**0*] has defining length = 4 because positions 1 and 5 are the first and last *fixed* alleles (5 – 1 = 4).

The Schema Theorem mathematically predicts the *minimum* copies of a specific schema in the current generation (t) that appear in the next generation (t +1). According to the Theorem, schemata with 1) short defining length 2) low order and 3) high fitness "receive exponentially increasing trials in subsequent generations" (Goldberg, 1989:33). These short, low-order, high-fitness schemata are called **building blocks**. An extension of the Schema Theorem is the Building Block Hypothesis, which states that a GA "seeks near optimal performance through the juxtaposition of short, low-order, high-performance schemata, or building blocks" (Goldberg, 1989:41). As the GA repeats the generation loop, building blocks accumulate exponenetially (Holland, 1992:180).

Although the Schema Theorem provides insight, it unfortunately provides an *inexact* schema count in the next generation because it is based on an inequality (≥); hence, the Schema Theorem predicts a *minimum* schema count with no provision for a maximum,

and it cannot accurately predict how a certain schema is processed as generations progress (Whitley, 1994).

Before using a GA to solve a problem, one must consider the following:

- A GA does not guarantee a globally optimum solution. Recall that a GA examines the search space probabilistically, not deterministically, so the optimum solution may be overlooked.
- Constraint handling is a challenge for GAs. If a chromosome (solution) violates any constraint, then it is infeasible and theoretically has zero fitness. However, this situation causes problems. In practice, problems incur many constraints, and "finding a feasible point is almost as difficult as finding the best" (Goldberg, 85:1989). As a result, the problem solver wants to make use of infeasible chromosomes because they may contain useful information (Goldberg, 85:1989; Coley, 72:1999). Goldberg (1989) identifies the "penalty method" as a means of retaining infeasible solutions. In the penalty method, an infeasible solution is allowed to have fitness, but its fitness degrades proportionally to its constraint violation (85). As Coley (1999) points out, "the form of the penalty function must be chosen with care" (72).
- According to Beasley (1993), "*convergence* is the progression towards increasing uniformity" (60), and premature convergence is a classic problem with GAs. In premature convergence, individuals with relatively high, but not the best, fitness rapidly dominate the population, causing the population to converge to a local maximum. As virtually identical strings continue reproduction and crossover, the

population becomes homogeneous, and continued search efforts become futile (Beasley, 64, 1993).

- Fitness evaluation of all chromosomes is undoubtedly the most time-intensive portion of the GA. Because a GA operates on a *population* of candidate solutions, it incurs the burden of evaluating the entire population; therefore, the evaluation function "must also be relatively fast" (Whitley, 1994). Extreme computational effort may necessitate networking processor hardware (Coley, 84-85:1999).

Assigning sensible values for internal GA parameters like crossover probability, mutation probability, and generation size is a dubious task because there are "no conclusive results on what is best" (Mitchell, 1996:175). Appropriate parameter values depend upon the nature of the problem (Coley, 22:1999).

2.6 PARETO-BASED MULTI-OBJECTIVE GENETIC ALGORITHMS

This section ties together sections 2.4 and 2.5 to introduce the multi-objective genetic algorithm (MOGA). In particular, this section focuses on MOGAs that use Pareto-based approaches.

The reader is reminded that all MOGAs are stochastic search algorithms based upon probabilistic methods. Because they are not deterministic, MOGAs can only generate an approximated, incomplete version of P* rather than P* itself. Therefore, the goal of a Pareto-based MOGA is convergence of P_{known} towards P*. MOGAs, like single-objective GAs, operate on a population of candidate solutions (chromosomes) as

opposed to a single solution; therefore, the strength of an MOGA is its ability to uncover *multiple* nondominated solutions (P_{known}) in a single run.

MOGAs differ from single-objective GAs in two fundamental ways:

- Solutions quantity. A single-objective GA typically searches for a *single* solution that best optimizes a single objective function. A MOGA, however, searches for *multiple* solutions that are Pareto-optimal.
- Fitness assignment. A single-objective GA assigns higher fitness to solutions that yield better performance relative to a single objective. However, MOGAs operate on two or more conflicting objectives; therefore, Pareto-dominance is the only basis for assigning fitness (Fonseca and Fleming, 1995:46).

2.6.1 Sorting nondominated solutions

Solutions exhibit various degrees of nondomination relative to each other. For example, for any two feasible solutions $\mathbf{x}_1$ and $\mathbf{x}_2$, the following scenarios are possible:

- Solution $\mathbf{x}_1$ dominates $\mathbf{x}_2$
- Solution $\mathbf{x}_2$ dominates $\mathbf{x}_1$
- Neither solution dominates the other

Because nondomination typically influences selection in MOGAs, there is a need to sort, or rank, chromosomes according to their degree of nondomination. Veldhuizen and Lamont (2000) point out that MOGAs typically rely on the ranking schemes of Goldberg (1989) and Fonseca and Fleming (1993). With the Goldberg (1989) method, the MOGA initially identifies nondominated chromosomes within the current population, assigns

them rank = 1, and removes them from the population. Next, the MOGA identifies nondominated chromosomes in the *remaining* population, assigns them rank = 2, and removes them from the population. This cycle of identification, ranking, and removal continues until all chromosomes in the current population are ranked. Reproductive probabilities are then based on rank (Goldberg, 1989:201).

The Fonseca and Fleming (1993) method is somewhat different. Suppose **x** is a particular chromosome in the current population. Then **x** receives rank = 1+ p, where p is the number of chromosomes in the *entire* current population that dominate **x**. Like Goldberg's (1989) method, the Fonseca and Fleming (1993) method ensures all nondominated chromosomes in the current population have rank = 1. However, while Goldberg's (1989) method successively removes individuals after ranking them, the Fonseca and Fleming (1993) method retains all chromosomes in the current population to be ranked among each other simultaneously.

2.6.2 Maintaining diverse solutions

In solving MOPs, Pareto-optimality is an essential property of any solution, but this alone is not sufficient. A secondary requirement is that solutions reflect sufficient diversity. Diversity can apply to either the solutions themselves (P*) or to their evaluation (PF*). This discussion, however, assumes that solution phenotype is more important than solution genotype, and, therefore, limits discussion of diversity to PF*, which reflects how solutions perform with the objective functions. A MOGA may generate thousands, or even millions, of Pareto-optimal solutions, but if they all converge

to the same portion of PF*, the large solution quantity yields no benefit for the decision maker.

Pareto-based MOGAs assign nondominated chromosomes equal fitness, which theoretically means they all have equal opportunity for reproduction. In practice, however, this is not the case because a GA operates on a *finite* population as opposed to an *infinite* population. Repetitious sampling of small, finite populations causes stochastic errors to accumulate. Consequently, even when multiple solutions offer no advantage over each other, the population ultimately converges to a single solution (Goldberg & Richardson, 1987:41-42). Such convergence due to stochastic errors from repeatedly sampling small population sizes is called *genetic drift* (Goldberg, 1989:185-186). Genetic drift causes MOGAs to eventually converge to a single nondominated solution (Fonseca and Fleming, 1993:6/2), which results in "crowding" (convergence) on the Pareto-front and loss of diversity. Goldberg and Richardson (1987) demonstrated genetic drift with single-objective GA optimizing a function with multiple optima or "peaks" (i.e., multimodal function). To counteract genetic drift, Goldberg and Richardson (1987) developed the idea of **fitness sharing**.

Fitness sharing is fundamentally driven by a parameter called the niche radius, σ_{share}. The parameter σ_{share} is a user-defined, radial distance that defines a circular **niche** around each point in objective space. Points that lie within σ_{share} of each other "share" the same niche and degrade each other's fitness (i.e. they must "share" each other's fitness). To determine the degraded/shared fitness of chromosome $\mathbf{x}_i$ due to nearby points in its niche, a **sharing function** is used. Goldberg and Richardson (1987) identify the following sharing function:

$$\begin{aligned} Sh(d_{ij}) &= 1 - (d_{ij} / \sigma_{share})^{\alpha} && \text{if } d_{ij} < \sigma_{share} \\ &= 0 && \text{otherwise} \end{aligned} \qquad (2.11)$$

Equation 2.11 depends upon parameters σ_{share} and α. The argument d_{ij} is the distance in objective space between $\mathbf{x}_i$ and some other chromosome $\mathbf{x}_j$; $\mathbf{x}_j$ can be a member of the entire population, a member of the same equivalence class as $\mathbf{x}_i$, or some other user-defined subset. The **niche count** m_i of chromosome $\mathbf{x}_i$ is the summation of its sharing function values with each chromosome $\mathbf{x}_j$:

$$m_i = \sum_{\mathbf{x}_j} Sh(d_{ij}) \qquad (2.12)$$

The niche count m_i quantifies the magnitude of crowding around chromosome $\mathbf{x}_i$ in objective space. Finally, the fitness of $\mathbf{x}_i$ is degraded ("shared") by dividing its original fitness f_i by its niche count m_i; shared fitness = f_i / m_i. Probabilities for selection are then based upon the shared fitness values (Goldberg and Richardson, 1987).

In MOGAs, fitness sharing can resolve the dilemma of how to select equal-ranking chromosomes. For example, a MOGA may initially assign equal fitness values to all chromosomes of some rank = k. To encourage diversity, the MOGA reduces fitness of each k-ranking chromosome in proportion to its niche count. These adjusted fitness values then guide selection. It is also possible to implement fitness sharing without directly adjusting chromosome fitness (Horn *et al*., 1994).

2.6.3 Mating restriction.

Arbitrary recombination of chromosome pairs having extreme dissimilarities (genotypic or phenotypic) may result in low-performance offspring called "lethals" (Goldberg, 1989:184). Therefore, it makes sense to restrict crossover to chromosome

pairs that are similar. As Goldberg (1989) points out, the sensibility of this restriction follows from nature, which prohibits mating among different organisms (mammals, birds, reptiles, etc.). Restriction of crossover among chromosome pairs is called **mating restriction**.

The purpose of mating restriction in MOGAs is to prevent creation of chromosomes that are not Pareto-optimal. Mating restriction within MOGAs is more relevant to phenotype than genotype due to greater interest in generating the Pareto front (Veldhuizen and Lamont, 2000). The distance parameter σ_{mate} controls mating restriction; chromosome $\mathbf{x}_i$ cannot crossover with other chromosomes that reside more than σ_{mate} from $\mathbf{x}_i$ in objective space. If a MOGA uses both fitness sharing and mating restriction, the common practice is to set $\sigma_{share} = \sigma_{mate}$, although such practice is purely arbitrary. No sound theory justifies the inclusion/exclusion of mating restriction in MOGAs (Veldhuizen and Lamont, 2000).

2.6.4 Pareto-based MOGAs in the literature.

Horn *et al*. (1994) developed the niched Pareto genetic algorithm (NPGA), which uses Pareto domination tournaments and fitness sharing chromosome selection. The NPGA creates a tournament by randomly picking two solutions $\mathbf{x}_1$ and $\mathbf{x}_2$ from the current population and by randomly filling a secondary population (the **comparison set**) with solutions; the comparison set is so-named because both $\mathbf{x}_1$ and $\mathbf{x}_2$ are compared to each member of the comparison set. If the comparison set dominates $\mathbf{x}_1$ but not $\mathbf{x}_2$, then $\mathbf{x}_2$ "wins the tournament" and is selected for reproduction. If the comparison set either

(a) dominates both $\mathbf{x}_1$ and $\mathbf{x}_2$ or (b) dominates neither $\mathbf{x}_1$ nor $\mathbf{x}_2$, then the tournament ends in a tie. In the case of a tie, it is probable that $\mathbf{x}_1$ and $\mathbf{x}_2$ belong to the same equivalence class, or partial order. The NPGA resolves ties with **equivalence class sharing**. In equivalence class sharing, the NPGA plots each solution in objective space and uses the user-defined parameter σ_{share} to assess crowding of adjacent points. Horn *et al*. (1994), however, defines niche count differently than equation 2.12. With the NPGA, the niche count m_i of chromosome $\mathbf{x}_i$ simply equals the count of points within σ_{share} of $\mathbf{x}_i$ in objective space. The NPGA ultimately selects either $\mathbf{x}_1$ or $\mathbf{x}_2$ based on lowest niche count (i.e. least crowded in objective space).

Srinivas and Deb (1994) introduced the nondominated sorting genetic algorithm (NSGA), so-named because it is based on a nondominated sorting procedure. The key features of the NSGA are 1) a ranking selection method to emphasize favorable solutions and 2) fitness sharing to form niches. The NSGA first identifies nondominated chromosomes in the current population and assigns them rank = 1. The NSGA initially assigns the same "dummy" fitness value to these rank-1 chromosomes. The NSGA employs fitness sharing by dividing each rank-1 chromosome's fitness by its niche count, calculated with equations 2.11 (α=2) and 2.12. The NSGA then separates the rank-1 chromosomes from the population, identifies nondominated chromosomes in the remaining population, assigns them the next rank (rank = 2), and gives them all the same fitness value, which is less than the minimum shared fitness of the previous rank (or "front"). Hence, the NSGA uses the Goldberg (1989) ranking method. The process of identifying nondominated solutions, assigning next rank, and adjusting fitness repeats for all chromosomes. The adjusted fitness values determine selection probabilities.

Deb *et al*. (2002) developed the Non-dominated Sorting GA-II (NSGA-II) to rectify flaws of the original NSGA of Srinivas and Deb (1994). Deb *et al*. (2002) identifies three key flaws with NSGA, which are 1) high computational complexity of nondominated sorting, 2) lack of elitism, and 3) reliance on user-specified σ_{share}

To improve nondominated sorting, NSGA-II compares each solution in the current population P with a partially-filled population (P') of nondominated solutions rather than the entire P. Comparing members of P with P' instead of the entire P itself has good potential for reducing the number of comparisons that the algorithm must check. NSGA-II, like NSGA, uses the Goldberg (1989) ranking method with nondominated fronts sequentially ranked and removed from P.

Deb *et al*. (2002) criticized NSGA's fitness sharing because of its reliance on the user chosen parameter σ_{share}. Computational burden is apparent in equations 2.11 and 2.12; NSGA must calculate phenotypic distances between chromosome $\mathbf{x}_i$ and every $\mathbf{x}_j$ in the same front and then evaluate the sharing function for all these distances. Also, the utility of equation 2.11 is sensitive to σ_{share} chosen by the user.

To overcome these problems, Deb *et al*. (2002) developed a fitness-sharing procedure that minimized the need for distance calculations and did not require specification of a niche radius parameter. NSGA-II sorts the population in ascending order using each series of objective function values. Boundary points (minimum and maximum) are assigned infinite crowding distance since they lack an adjacent neighbor. For each intermediate point i, NSGA-II computes only two crowding distances: the distances between i and its two adjacent neighbors. The overall crowding distance value of point i equals the sum of individual distance values associated with each objective.

The disadvantage of this procedure is the computational burden of sorting points for each series of objective function values (Deb *et al*., 2002).

The main loop of NSGA-II works as follows: NSGA-II combines the parent and children populations and sorts/ranks the combined population using the improved nondominated sorting procedure explained earlier. Next, the algorithm computes crowding distances for each front. NSGA-II fills an *N*-size mating pool with priority given to lower-ranking chromosomes; in this regard, NSGA-II uses an elitist method. When the algorithm encounters a particular front/rank whose members exceed space left in the pool, the algorithm resorts to fitness sharing. NSGA-II picks chromosomes from the front that have the lowest crowding distances. The filled mating pool undergoes crossover and mutation to create a new population of children of size *N* (Deb *et al*., 2002).

Zitzler and Thiele (1998) developed the strength Pareto evolutionary algorithm (SPEA) which combines traditional and new MOGA techniques to find nondominated solutions. SPEA starts by initializing a population (P) and an *external dominated set* (P'), which is initially empty. The algorithm copies nondominated chromosomes from P to P' and removes chromosomes from P' that are dominated by any other member of P'. A specified size parameter (N') limits the number of nondominated chromosomes that P' can store, and a clustering technique known as the average linkage method is used to "prune" (remove) excess chromosomes from P'. SPEA then computes "strength" (fitness) for each $\mathbf{x}_i \in P'$ by computing a strength value (s_i) that is directly proportional to the number of chromosomes in P' that $\mathbf{x}_i$ dominates. SPEA also computes a strength

value (s_j) for each $\mathbf{x}_j \in P$ by summing the strength values of all chromosomes in P' that dominate $\mathbf{x}_j$. Zitzler and Thiele (1998) reverse the meaning of "fitness" within SPEA because higher reproductive probabilities correspond to *lower* fitness/strength as opposed to higher fitness. Furthermore, the SPEA niching technique defines niches in terms of Pareto dominance instead of phenotypic distance, which eliminates the need for a user-specified distance parameter (i.e. σ_{share}). SPEA uses binary tournament selection with replacement to copy chromosomes from both populations ($P \cup E$) to the mating pool. Once full, chromosomes in the mating pool undergo problem-specific crossover and mutation, which completes a generation.

Van Veldhuizen (1999) developed the "messy" multiobjective genetic algorithm (MOMGA), which differs from the previous MOGAs in that MOMGA principally operates on *building blocks* (BBs) (see Section 2.5) instead of whole chromosomes. MOMGA consists of three distinct phases: (1) initialization, (2) primordial phase, and (3) juxtapositional phase. In the initialization phase, MOMGA uses Partially Enumerative Initialization (PEI) to initialize a population representing all possible BB variations of specific size. Following PEI, building blocks are evaluated with respect to a competitive template, and then MOMGA performs subroutines for the primordial and juxtapositional phases. In the primordial phase subroutine, Pareto-based tournament selection repeatedly adjusts the size of the current BB population. In the juxtapositional phase, MOMGA clones desired BBs and recombines them into complete chromosomes using a "cut-and-splice" operator. New chromosomes are subsequently evaluated against the competitive template and, if they are currently Pareto optimal, they are added to the currently Pareto optimal set. Once the juxtapositional loop ends, MOMGA updates the competitive

template using the best fitness values. MOMGA then executes another cycle of initialization, primordial, and juxtapositional phases (Van Veldhuizen, 1999).

The disadvantage of MOMGA lies in the PEI, which deterministically enumerates all possible BB clones and, consequently, incurs significant computational expense (Zydallis *et al*., 2001). MOMGA-II, developed by Zydallis *et al*. (2001), is similar to MOMGA with some notable exceptions. MOMGA-II uses Probabilistically Complete Initialization (PCI) instead of PEI to initialize a limited-size BB population, which effectively reduces computational "bottlenecks." Also, instead of a primordial phase, MOMGA-II implements a Building Block Filtering (BBF) phase to probabilistically ensure that all desirable BBs are in the initial population. BBF essentially reduces the number of BBs and stores the best BBs found (Zydallis *et al*., 2001).

3.0 METHODOLOGY

3.1 INTRODUCTION

In this chapter, we describe the procedures used to achieve our research objective of determining values of design variables that optimize technology cost and performance under various contaminated-site conditions. In Section 3.2 of this chapter, we present the details of Parr's (2002) technology model for remediating perchlorate contamination using HFTWs in conjunction with *in situ* biodegradation. In Section 3.3, we establish parameter values to describe an actual perchlorate-contaminated site. In Section 3.4, we formulate a multi-objective optimization problem, establishing objective functions for application of the remediation technology at the site. In Section 3.5 we present a multi-objective GA (MOGA) that is used to solve the optimization problem. Finally, in Section 3.6, we describe the details of implementing the MOGA.

3.2 TECHNOLOGY MODEL

Parr (2002) developed a technology model that combines groundwater flow and transport of dissolved species induced by operation of an HFTW system with a bioremediation submodel that simulates perchlorate reduction due to introduction of an electron donor in the HFTW treatment wells. In this section, we describe both the flow-and-transport model and the bioremediation submodel implemented in this study.

3.2.1 Flow and Transport Model

Parr (2002) adapted the Huang and Goltz (1998) numerical model, which was originally used for TCE, to simulate flow and transport of ClO_4^- in groundwater flow fields induced by a 2-well HFTW system. The 3-D flow-and-transport model is a numerical model that simulates advection, dispersion, and consumption of four individual, dissolved species (electron donor, oxygen, nitrate, and perchlorate). Consumption rates of dissolved species are due to microbially mediated redox reactions, and rate equations for these reactions are in the biological submodel (section 3.2.2). The flow-and-transport model assumes only the electron donor (acetate CH_3COO^-) can sorb, and this sorption is assumed to be an equilibrium process that is both linear and reversible. The remaining species (O_2, NO_3^-, ClO_4^-) are non-sorbing. Parr (2002) further assumes microorganisms remain stationary (i.e. fixed to the aquifer material). The flow-and-transport model equations are presented in Appendix A.

The flow-and-transport model is coded in FORTRAN. MODFLOW (Harbaugh and McDonald, 1996), which is a three-dimensional finite difference code, is used as a subroutine to calculate groundwater flow, as the model transport equations (A.1-A.4) require groundwater flow velocities (v) throughout the problem domain as input. Given boundary conditions for hydraulic head (h), along with values for aquifer hydraulic conductivity (K), porosity (n), HFTW treatment well locations, and treatment well pumping rates, MODFLOW solves the steady-state flow equation (3.1) to determine the hydraulic head field and then applies Darcy's law (3.2) to compute the steady-state velocity field in three dimensions.

$$\nabla^2 h = 0 \qquad (3.1)$$

$$v = \frac{-K}{n}\nabla h \qquad (3.2)$$

The flow-and-transport model separately accepts other input information, like injected donor concentration and injection frequency. After accepting the three dimensional steady-state groundwater flow velocity input from MODFLOW, along with initial/boundary concentrations of the dissolved species and microbes, the flow-and-transport model uses a self-adaptive, partial implicit finite difference technique to numerically solve the partial differential equations describing advection, dispersion, sorption, and consumption in Appendix A. The model can provide concentrations for all species (electron donor, electron acceptors, and microorganisms) at any location over time.

3.2.2 Biological Treatment Submodel

Parr (2002) based his biological treatment submodel on a perchlorate biodegradation model developed by the environmental firm Envirogen. The biological treatment submodel model consists of differential equations, based on dual-Monod kinetics, that describe 1) consumption rates of dissolved species (electron donor, oxygen, nitrate, perchlorate) due to microbial redox reactions, and 2) biomass changes. A notable feature of the submodel is that it addresses the competition among multiple electron acceptors for oxidation of the electron donor; the submodel assumes that oxygen is preferentially reduced over nitrate, which is preferentially reduced over perchlorate. The

reader may refer to Appendix A for a more detailed discussion of the submodel equations.

3.3 SITE MODEL

Applying a technology model to simulate remediation at an actual contaminated site necessitates translating the site characteristics into model parameters. Using a pre-processor such as the one available in Visual MODFLOW, a grid composed of discrete, rectangular cells can be easily constructed to approximate a perchlorate-contaminated site. A key advantage of the Visual MODFLOW pre-processor and the MODFLOW code is that they allow the user to represent the site with non-uniform cell sizes. The user can specify smaller, numerous cells for better resolution in the vicinity of pumping wells and treatment wells; and the user can conversely specify larger, fewer cells in less critical areas to reduce computational time. Using the pre-processor, the user can locate pumping and injection wells anywhere in the finite difference grid, establish head and concentration boundary conditions, contaminant concentration initial conditions, and specify hydrogeological characteristics. Site information is saved to data files that are later read by MODFLOW.

A plan view of the site is shown in Figure 3.1. This finite difference, composite grid is actually 3-dimensional, 185 m long by 185 m wide by 32 m deep. This grid is a composite of discrete, rectangular cells of non-uniform size. Individual cells have sides of 3 m, 5 m, or 10 m. More numerous, smaller cells (3 m × 3 m) are located within the vicinity of the pumping wells for better resolution. Larger cells (10 m × 10 m) are

specified at the extremities of the grid, where resolution is less important, to reduce computational time. This grid has four layers with a uniform horizontal hydraulic conductivity that is twenty times greater than the vertical conductivity. This anisotropy is assumed constant over the entire modeled volume. The top layer represents an 8 meter deep zone, where the water table is located an average of 1.5 meters below the surface. The second and fourth layers (10 meters deep each) are where the upper and lower screens of the treatment wells are located, and the third layer (4 meters deep) separates the screened intervals.

Two treatment wells are oriented perpendicular to the direction of groundwater flow, which is left to right in Figure 3.1. The configuration in Figure 3.1 is used to evaluate how well a pair of HFTWs can be used to contain a perchlorate plume from being transported downgradient from a continuous source.

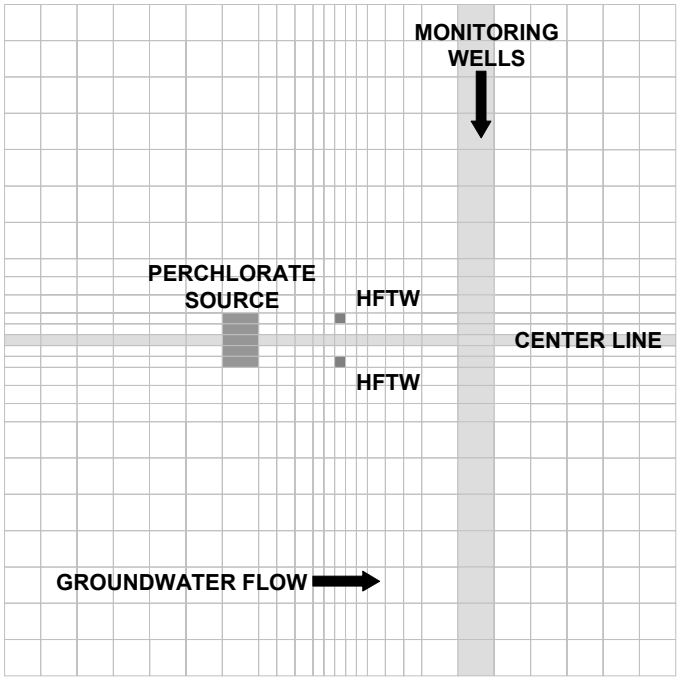

Figure 3. Contaminated site model – aerial view.

3.4 FORMULATION OF MULTI-OBJECTIVE PROBLEM

Having developed a technology model and a site model, we are now in a position to formulate a multi-objective problem. Over a given time of technology operation, we wish to 1) destroy as much perchlorate as possible and simultaneously 2) keep operating costs of the remediation technology low. These objectives can be represented as f_1 and f_2, respectively. Next, we must identify characteristics (decision variables) that a site engineer could manipulate to pursue these objectives. Such characteristics are

Q = pump rate (m^3/day) for each well in the HFTW well pair

d = spacing between the two treatment wells in the well pair (meters)

C_{in} = injected concentration of acetate (mg/L)

p = acetate injection pulse duration (in 32^{nds} of a day)

We now want to mathematically express the objectives f_1 and f_2 as functions of the decision variables. However, objective f_1 (mass perchlorate destroyed) cannot be explicitly written as a function of the decision variables. Looking at the technology model, we can see that f_1 is a function of the decision variables, but determining f_1 for a given set of decision variable values requires numerical evaluation of the set of partial differential equations that comprise the technology model. Therefore, we generically represent objective f_1 as

$$\text{Mass } ClO_4^- \text{ destroyed} = f_1(Q, d, C_{in}, p)$$

On the other hand, the relationship between f_2 (total operating cost) and $[Q, d, C_{in}, p]$ can be explicitly formulated. To simplify our comparison of operating costs for different implementations of the remediation technology, we assume that operating cost

differences are only due to differences in the a) cost of electron donor and b) cost of operating the pumps. That is, we implicitly assume that capital costs, as well as other recurring costs (*e.g.* maintenance) for different technology implementations are equal.

Cost of electron donor depends upon how much electron donor is injected over the duration of the remediation period t, and we can write this cost as

$$\text{Material cost} = 2^* Q * t * C_{in} * p/32 * 1000 \text{ L/m}^3 * Price_{donor}, \text{ where}$$

2 = number of treatment wells

t = treatment period (days)

32 = maximum pulse duration (32 pulse units = 1 day)

1000 L/m^3 = conversion factor

$Price_{donor}$ = price of electron donor injected ($/mg donor)

The remediation technology also incurs the cost of operating the pumps in the two HFTWs. Assuming continuous pump operation, the pump cost equation becomes

$$\text{Pump cost} = 2^* Q * t * E * Price_{elec}$$

where

2 = number of treatment wells

E = energy required to overcome headloss (kW-hr per m^3 of water; see appendix B)

$Price_{elec}$ = price of electricity ($/kW-hr)

We can now explicitly write objective f_2 as a function of decision variables:

$$\text{Operating cost} = \text{Material cost} + \text{Pump cost}$$

$$f_2(Q, C_{in}, p) = 2^* Q * t * C_{in} * p/32 * 1000 \text{ L/m}^3 * Price_{donor} + 2^* Q * t * E * Price_{elec}$$

$$f_2(Q, C_{in}, p) = 2^* Q * t * (C_{in} * p/32 * 1000 \text{ L/m}^3 * Price_{donor} + E * Price_{elec})$$

Finally, we must recognize the constraints that our problem domain imposes. The site and technology models impose lower and upper bounds on each of the decision variables which we can designate as Q_{min}, Q_{max}, d_{min}, d_{max}, $C_{in,min}$, $C_{in,\,max}$, p_{min}, and p_{max}.

With our objectives, decision variables, and constraints identified, we can now formulate a multi-objective problem: search for all vectors $\mathbf{x} = [Q, d, C_{in}, p]$ that optimize the objective function vector $\mathbf{f}(\mathbf{x}) = [f_1(\mathbf{x}), f_2(\mathbf{x})]$ subject to the following constraints:

$$Q_{min} \leq Q \leq Q_{max}; \text{ real-valued}$$

$$d_{min} \leq d \leq d_{max}; \text{ integer-valued}$$

$$C_{in,min} \leq C_{in} \leq C_{in,\,max}; \text{ real-valued}$$

$$p_{min} \leq p \leq p_{max}; \text{ real-valued.}$$

For this problem, HFTW placement is restricted to cells in column 13 of the finite difference grid shown in Figure 3.1; furthermore, the two HFTWs are required to remain equidistant from the grid centerline. Hence, when looking at Figure 3.1, well-spacing (d) is the vertical grid distance between HFTWs. Note that d must be integer because it measures the summation of vertical cells between the HFTWs, and individual cell dimensions are integer (3, 5, or 10 meters). The remaining decision variables (Q, C_{in}, p), however, can accommodate better resolution than integer values, and therefore, are designated as real.

The objective of this problem is to find sets of engineering parameters [Q, d, C_{in}, p] that yield an optimal trade-off relationship between technology performance (with respect to perchlorate removal) and cost. Ideally, we would further constrain the solution set to values [Q, d, C_{in}, p] that yield downgradient ClO_4^- concentrations that fall below some maximum level; the rationale for this constraint is that regulations typically

prescribe a maximum contaminant level downgradient from the source. However, the ability of the technology model to yield sufficiently low ClO_4^- levels is largely uncertain; this additional constraint would risk over-constraining the problem and yielding no solutions. Therefore, instead of formulating downgradient ClO_4^- concentration as an objective or constraint, we simply monitor downgradient ClO_4^- concentration to gain an understanding of how different technology implementations affect the relative magnitude of this important parameter.

There are some important considerations in selecting a suitable search algorithm to solve this problem:

- Objectives f_1 and f_2 have common decision variables [Q, C_{in}, p], but the mathematical relationship between f_1 and f_2 is unknown. In other words there is no analytical expression for the theoretical Pareto Front (PF*).
- An explicit relationship between f_1 and [Q, d, C_{in}, p] is unavailable.
- Because a discrete plot of the Pareto front is the only representation achievable, the plot must adequately span the extremities of the Pareto front.
- Due to the relatively long computation time in evaluating a decision variable set, an efficient search algorithm is essential.

Given these considerations, a genetic algorithm seems appropriate for estimating PF*. As stated in Section 2.5, GAs adapt easily to multi-objective problems because they operate on a population of candidate solutions, enabling the discovery of multiple nondominated points in a single generation.

3.5 MULTI-OBJECTIVE GENETIC ALGORITHM

3.5.1 MOGA specifications

In developing an MOGA to solve the proposed problem, the following MOEA characteristics are desireable:

- Pareto-based to generate discrete, approximated Pareto-optimal solutions.
- Real-valued crossover and mutation operators to accommodate possible ranges of values for the decision variables.
- Fitness sharing to generate points that adequately span the Pareto front.
- Parallelized to expedite computation by allowing multiple processors to individually calculate fitness for a particular chromosome. Parallelization is a practical necessity due to computation intensity of computing the FORTRAN flow-and-transport model.

Section 2.6 described several multi-objective GAs. For this thesis effort, the author implemented a version of NPGA largely due to its success in previously solving a multi-objective groundwater remediation problem that is somewhat similar to the problem being considered here (Erickson *et al*., 2001). Also, the author considered NPGA easily understandable and easiest to develop into low-level computer code. From this point, forward, the algorithm will be referred to as HK-MOGA, in which the letters H and K refer to the software developers (Hendricks and Knarr; see Acknowledgments).

3.5.2 Chromosome encoding

A chromosome consists of genes representing the decision variables listed in Section 3.4. In essence, a chromosome contains engineering parameters for a 2-well HFTW system. Chromosomes also have auxiliary genes devoted to objective function values, Pareto-ranking, and downgradient ClO_4^- concentration, but these auxiliary genes are not involved in crossover or mutation. Decision variables are real-valued except for well-spacing, which is integer-valued.

3.5.3 MOGA parameters

HK-MOGA relies on the following user-specified parameters:

- Initial population size ($|Pop_0|$): self-explanatory
- Mating pool size ($|MP|$): sets the quantity of chromosomes that are selected for crossover and mutation.
- Number of generations (N): determines how many cycles of selection, crossover, and mutation occur.
- Niche radius (σ_{share}): dimensionless number used in fitness sharing; establishes a circular niche around each point in non-dimensionalized objective space
- Mutation probability (p_m): self-explanatory

3.5.3 Initialization

HK-MOGA starts by randomly generating an initial chromosome population Pop_0 of size $|Pop_0|$ in which all chromosomes comply with decision variable constraints listed

in section 3.4. HK-MOGA stores the created chromosomes in a set called Pop_{cum} , so-called because it is a cumulative collection of chromosomes; HK-MOGA continually appends newly generated chromosomes to Pop_{cum}.

After Pop_{cum} is created, HK-MOGA evaluates objective function values for each chromosome. HK-MOGA next uses the objective function values to Pareto-rank each chromosome in Pop_{cum}. A particular chromosome **x** receives a rank that equals the number of chromosomes that dominate chromosome **x**. Hence, all nondominated solutions have rank = 0, and low rank corresponds to high fitness. This Pareto-ranking method mimics the method of Fonseca and Fleming (1993).

3.5.4 Selection

Once chromosomes are Pareto-ranked, HK-MOGA starts the generation subroutine, which begins by selecting chromosomes to be copied to a reservoir called a mating pool (*MP*) where they await crossover and mutation. The user-specified parameter |*MP*| limits the number of chromosomes in *MP*.

Two properties that drive selection in HK-MOGA are 1) Pareto rank and 2) "crowding" in objective space. As long as space in *MP* is sufficient, HK-MOGA copies all rank-zero chromosomes to *MP*, then all rank-1's, then all rank-2's, etc. Simply put, when space is sufficient, Pareto rank drives selection. This method ensures that better, low-ranking chromosomes receive priority for selection.

However, as low-ranking chromosomes are progressively copied, space in *MP* depletes. Eventually HK-MOGA encounters chromosomes of some rank *k* whose quantity exceeds remaining space. Because all *k*-rank chromosomes have equal rank, and

therefore fitness, HK-MOGA resolves the dilemma of which chromosomes to select by picking chromosomes that are least crowded in objective space. The purpose of this selection strategy is to develop chromosomes that map to relatively uninhabited sections of the Pareto front, which for the decision maker means more diverse tradeoff options. The metric for assessing crowding in objective space is the niche count. This technique is called **equivalence class sharing**, which was originally described by Horn *et al*. (1994).

Let $\mathbf{x}_i$ be some *k*-rank chromosome such that i = 1, 2, 3…[number of rank *k* chromosomes], and assume that the number of *k*-rank chromosomes exceeds remaining space in the mating pool. Also, let chromosome $\mathbf{x}_j$ be any chromosome in Pop_{cum} where j = 1, 2, 3…[size of Pop_{cum}]. HK-MOGA searches Pop_{cum} for the most current maximum and minimum values of both objective functions f_1 and f_2. These maximum and minimum values are subsequently used to normalize objective function values for every $\mathbf{x}_i \in$ {rank *k* chromosomes} and $\mathbf{x}_j \in Pop_{cum}$ as follows:

$$f_1'_i = (f_{1i} - f_{1min}) / (f_{1max} - f_{1min})$$

$$f_2'_i = (f_{2i} - f_{2min}) / (f_{2max} - f_{2min})$$

$$f_1'_j = (f_{1j} - f_{1min}) / (f_{1max} - f_{1min})$$

$$f_2'_j = (f_{2j} - f_{2min}) / (f_{2max} - f_{2min})$$

where

$f_1'_i$ = dimensionless value of f_1 based on $\mathbf{x}_i \in$ {rank *k* chromosomes}

$f_2'_i$ = dimensionless value of f_2 based on $\mathbf{x}_i \in$ {rank *k* chromosomes}

$f_1'_j$ = dimensionless value of f_1 based on $\mathbf{x}_j \in Pop_{cum}$

$f_1'_j$ = dimensionless value of f_2 based on $\mathbf{x}_j \in Pop_{cum}$

f_{1i} = value of f_1 based on $\mathbf{x}_i \in$ {rank *k* chromosomes}

f_{2i} = value of f_2 based on $\mathbf{x}_i \in$ {rank *k* chromosomes}

f_{1j} = value of f_1 based on $\mathbf{x}_j \in Pop_{cum}$

f_{2j} = value of f_2 based on $\mathbf{x}_j \in Pop_{cum}$

f_{1min} = minimum value of f_1 within Pop_{cum}

f_{1max} = maximum value of f_1 within Pop_{cum}

f_{2min} = minimum value of f_2 within Pop_{cum}

f_{2max} = maximum value of f_2 within Pop_{cum}

This normalization makes both objective function values dimensionless, which is helpful due to the incommensurable units of both objective functions (mass and dollars). The distance d_{ij} between points $(f_1'_i, f_2'_i)$ and $(f_1'_j, f_2'_j)$ in dimensionless objective space is calculated as

$$d_{ij} = [\ (f_1'_i - f_1'_j)^2 + (f_2'_i - f_2'_j)^2\ ]^{½}$$

Distance d_{ij} and the niche radius σ_{share} are then used to compute the sharing function (equation 2.11):

$$Sh(d_{ij}) = 1 - d_{ij}/\sigma_{share} \qquad \text{for } d_{ij} \le \sigma_{share}$$

$$= 0 \qquad \text{for } d_{ij} > \sigma_{share}$$

The parameter σ_{share} basically defines the radius of a circle around point $(f_1'_i, f_2'_i)$; points inside the circle contribute to crowding, and points outside the circle do not. $Sh(d_{ij})$ is a

metric for assessing the proximity or crowding between point $(f_1'_i, f_2'_i)$ and some other point $(f_1'_j, f_2'_j)$. If $(f_1'_j, f_2'_j)$ lies within the circle surrounding $(f_1'_i, f_2'_i)$ (i.e. $d_{ij} \leq \sigma_{share}$), then the sharing function assumes a value such that $0 \leq Sh(d_{ij}) \leq 1$. The closer the two points are to each other, the higher the value of the sharing function; the maximum value $Sh(d_{ij}) = 1$ indicates the two points overlap. If point $(f_1'_j, f_2'_j)$ lies outside the circle surrounding $(f_1'_i, f_2'_i)$ (i.e. $d_{ij} > \sigma_{share}$), then crowding is negligible ($Sh(d_{ij}) = 0$).

The niche count m_i for chromosome $\mathbf{x}_i \in \{\text{rank } k \text{ chromosomes}\}$ is computed according to equation 2.12:

$$m_i = \sum_{\mathbf{x}_j \in Pop_{cum}} Sh(d_{ij})$$

Because m_i is a summation of sharing function values, it provides an overall measure of how "crowded" chromosome $\mathbf{x}_i$ is in objective space. A high niche count implies a high degree of crowding, and vice versa (see Figure 4). After calculating the niche count m_i for each $\mathbf{x}_i \in \{\text{rank } k \text{ chromosomes}\}$, HK-MOGA fills remaining slots in *MP* with chromosomes having the lowest m_i values. HK-MOGA preferentially selects chromosomes with low niche counts to improve chances of generating points in less-occupied regions of the Pareto front.

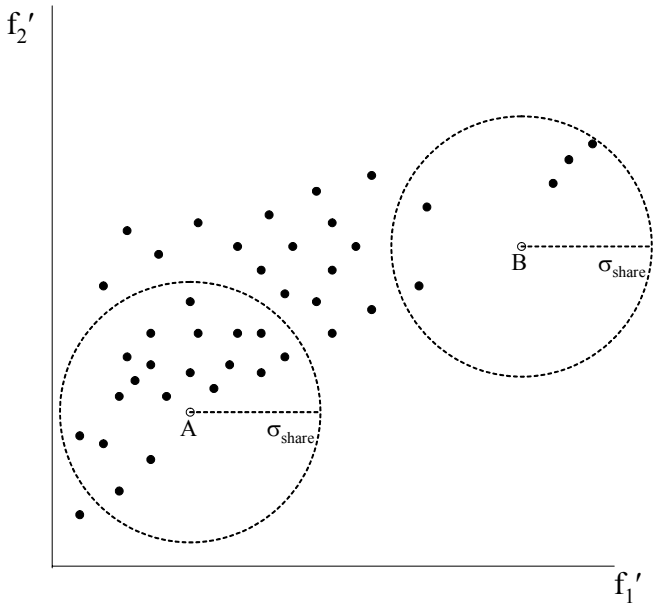

Figure 4. Example of niching strategy. Point B is less crowded than point A.

3.5.5 Crossover and Mutation

Chromosomes in *MP* proceed to crossover and mutation. HK-MOGA relies on several crossover/mutation operators, which Garrett (1999) coded for his thesis investigation. Garrett's (1999) computer code was incorporated into HK-MOGA code. Although Section 2.6.4 addresses mating restriction during crossover, mating restriction does not appear to be a critical component of MOGAs investigated in the literature review, and, as stated before, no sound theory justifies its inclusion in MOGAs (Veldhuizen and Lamont, 2000). Therefore, the author did not incorporate mating restriction with the crossover.

All chromosomes in *MP* participate in crossover. That is, for i = 1 to |*MP*|, chromosome $\mathbf{x}_i$ crosses over with $\mathbf{x}_r$, where $\mathbf{x}_r$ is randomly chosen from *MP* (pool crossover operates differently). HK-MOGA employs the following crossover operators:

Whole arithmetical crossover: linearly combines all corresponding genes of $\mathbf{x}_i$ and $\mathbf{x}_r$, to create new chromsomes $\mathbf{x}'_1$ and $\mathbf{x}'_2$; crossover applies to the "whole" chromosome (i.e. all genes of $\mathbf{x}_i$ and $\mathbf{x}_r$) (Michaelwicz, 1996:112, 128). HK-MOGA randomly retains $\mathbf{x}'_1$and discards $\mathbf{x}'_2$.

Simple crossover: randomly selects a gene and swaps it between $\mathbf{x}_i$ and $\mathbf{x}_r$ to make $\mathbf{x}'_1$ and $\mathbf{x}'_2$ (Michaelwicz, 1996:112). HK-MOGA randomly retains $\mathbf{x}'_1$and discards $\mathbf{x}'_2$.

Heuristic crossover: uses chromosomes $\mathbf{x}_i$ and $\mathbf{x}_r$ to make a single offspring $\mathbf{x}'_1$ such that $\mathbf{x}'_1 = R\cdot(\mathbf{x}_r - \mathbf{x}_i) + \mathbf{x}_r$. The value R is a uniform random number between 0 and 1, and the rank of $\mathbf{x}_r$ is the same or less than the rank of $\mathbf{x}_i$ (Michaelwicz, 1996:112).

Pool crossover: randomly copies alleles from chromosomes in *MP* and assembles the alleles to make $\mathbf{x}'_1$.

HK-MOGA selects a particular crossover operators based upon an adaptive probability distribution (Garrett, 1999). At the first generation, all crossover operators have equal probability of selection. For all following generations, the selection probability for a particular operator "adapts" or adjusts based upon the attributes of the new chromosome $\mathbf{x}'_1$. If $\mathbf{x}'_1$ dominates $\mathbf{x}_i$, then the crossover operator was successful in increasing fitness, and its selection probability consequently increases in the next generation. Conversely, if $\mathbf{x}_i$ dominates $\mathbf{x}'_1$, then crossover was unsuccessful, and its probability of selection decreases. If neither chromosome dominates the other, the operator's selection probability stays the same.

Crossover creates new chromosomes that are then susceptible to mutation. Mutation is controlled by the user-specified mutation probability (p_m). For each new chromosome, HK-MOGA selects a random number (r: $0 < r < 1$) from a uniform distribution. If $r < p_m$, then one of 3 mutation operators affects the new chromosome; otherwise, mutation does not occur. HK-MOGA randomly selects which mutation operator based on the same adaptive probability distribution described previously:

Uniform mutation: resets a particular gene to a random value between specified maximum and minimum values (Michaelwicz, 1996:111, 127).

Boundary mutation: resets a particular gene to either its specified maximum or minimum value (Michaelwicz, 1996:127-128).

Non-uniform mutation: modifies a particular gene by some random value whose magnitude decreases probabilistically towards 0 as the current generation number approaches the maximum generation number (Michaelwicz, 1996:111, 128).

Crossover and mutation ultimately create a new chromosome population Pop_{new}, whose size equals the mating pool size $|MP|$.

3.5.6 Evaluation and Pareto Ranking

HK-MOGA evaluates all members of Pop_{new} and appends them to Pop_{cum}. Thus, Pop_{cum} keeps all chromosomes from past generations and inherits new ones. We see then that Pop_{cum} is a set of accumulated chromosomes, and its cardinality is prescribed by the following formula:

$$|Pop_{cum}| = N \cdot |MP| + |Pop_0|$$

HK-MOGA ranks each chromosome in Pop_{cum} as described previously, and the generation cycle restarts with selection.

3.6 OPTIMIZATION PROCEDURE

The author designed optimization runs to achieve the second and third objectives mentioned in Section 1.2. Four separate optimization runs were performed using HK-MOGA described in section 3.5 to produce an estimated Pareto set (P_{known}) and Pareto front (PF_{known}) for different time spans and site conditions. Runs 1 and 3 simulate treatment periods of 300 days and 600 days, respectively, using site data for Site 4, Nevada (Parr, 2002):

Aquifer Characteristics
Hydraulic Conductivity = 7.6 m/day Hydraulic Gradient = 0.01
Source Characteristics
Oxygen Concentration = 2.8 mg/L Nitrate Concentration = 60 mg/L
Perchlorate Concentration = 330 mg/L

Runs 2 and 4 simulate treatment periods of 300 days and 600 days, respectively, using site data for Site 2, California (Parr, 2002):

Aquifer Characteristics
Hydraulic Conductivity = 2.59 m/day Hydraulic Gradient = 0.001
Source Characteristics
Oxygen Concentration = 0.55 mg/L Nitrate Concentration = 0.5 mg/L
Perchlorate Concentration = 160 mg/L

As mentioned in Section 1.2, one of the research objectives was to perform the optimization under "various contaminated-site conditions." Key parameters that establish different conditions between the two sites are hydraulic conductivity, regional hydraulic

gradient and initial source concentration. Site 4 has approximately triple the hydraulic conductivity, ten times the hydraulic gradient, and double the source concentration of Site 2; Site 4 also has larger initial concentrations of competing electron acceptors (O_2 and NO_3^-) than Site 2.

The following parameters are used in all four runs:

Decision variable constraints
Q_{min} = 10 m^3/day Q_{max} = 150 m^3/day d_{min} = 3 m d_{max} = 165 m
$C_{in,min}$ = 0 mg/L $C_{in,\,max}$ = 1,000 mg/L
p_{min} = 0 p_{max} = 32
Cost coefficients
$Price_{donor}$ = \$2.666×10^{-6} per mg donor $Price_{elec}$ = \$0.067 per kW-hr
HK-MOGA parameters
|Pop_0| = 50 |*MP*| = 10 *N* = 100 σ_{share} = 0.4 p_m = 0.01
Aquifer parameters
Porosity = 0.30 Retardation factor for acetate (CH_3COO^-) = 1.48
Kinetic parameters (see Appendix A)
k_{max} = 0.21 mg donor/mg biomass/day K_S^{don} = 10.0 mg/L
K_S^{oxy} = 10.0 mg/L K_S^{nit} = 15.0 mg/L K_S^{per}= 20.0 mg/L
K_i^{oxy} = 10.0 mg/L K_i^{nit} = 15.0 mg/L
$Y_{biomass}$ = 0.25 mg biomass/mg donor
F_{oxy} = 0.83 mg oxygen/mg donor F_{nit} = 1.3 mg nitrate/mg donor
F_{per} = 1.45 mg oxygen/mg donor b = 0.002 day^{-1} X_{min} = 0.01 mg/L

The Q_{max} was selected as an appropriate real-world value that would not result in excessive drawdown at the sites. Values for d_{min} and d_{max} are based upon the dimensions of the site model. The value for $Price_{donor}$ is based upon an estimated bulk cost of \$286.20 per 55-gallons of a 50/50 mixture of acetic acid (CH_3COOH) and water. The value for $Price_{elec}$ came from a U.S Department of Energy (USDOE) website that lists average electricity prices for commercial consumers in Nevada in the year 2000 (USDOE, 2003). All values for the kinetic parameters are the same as the baseline values that Parr used (2002) except for the biomass decay rate, which was changed to a value of b = 0.002 day^{-1} (originally b = 0.01 day^{-1}) to simulate less biomass decay. HK-MOGA

parameters values are based on both knowledge of similar parameter values seen in the literature and off-line experiments with the HK-MOGA software.

The HK-MOGA software performs the evaluation function (Section 3.5.6) by executing the FORTRAN-coded technology model and computing the cost formula for each new chromosome. Execution of the technology model is the most computationally expensive and time-intensive activity in the program. HK-MOGA, which is coded in C++, uses Message-Passing Interface (MPI) to enable parallel computation among several Aspen dual-processor machines. Each Aspen machine has 1-GB memory and two 1-GHz Pentium III processors that can separately evaluate the technology model for each chromosome. Evaluations for 300-day and 600-day scenarios typically lasted about 8 and 17 minutes, respectively, on each processor. The program was executed with Redhat LINUX version 7.3 and MPI version 1.2.7.1.

In addition to decision variable and objective function values, the HK-MOGA software also outputs the maximum ClO_4^- concentration among all cell layers of column 20 of the finite difference grid (the monitoring wells shown in Figure 3). As mentioned before, the purpose of including this output is to assess the ability of the treatment technology to meet regulatory requirements.

4.0 RESULTS AND ANALYSIS

4.1 INTRODUCTION

In this chapter we present and discuss the results obtained from using HK-MOGA described in Section 3.5 to optimize both perchlorate-mass destruction and operating cost incurred based upon simulations of Parr's (2002) *in situ* bioremediation technology model. First we compare Runs 1 and 2 (300-day scenarios) for Sites 4 (in NV) and 2 (in CA) with respect to their estimated Pareto fronts (PF_{known}) and their downgradient perchlorate concentration ($[ClO_4^-]$) data. Next, a similar analysis is presented for Runs 3 (Site 4) and 4 (Site 2) for 600 days of technology operation.

4.2 RESULTS FOR 300-DAY TECHNOLOGY OPERATION

Figures 5 and 6 show PF_{known} for Runs 1 and 2, respectively, at generation N = 100. Each graph displays evaluations of ClO_4^- mass removal (f_1) and operating cost (f_2) assuming a 300-day time span. At N = 100, Runs 1 and 2 generated 429 and 461 nondominated points, respectively, out of a total of 1,050 points. For both runs, HK-MOGA discovered the same upper and lower extremities with respect to operating cost, and for both runs PF_{known} acquired sufficient definition (*i.e.* converged) by $N \approx 50$. The niching strategy described in Section 3.5.4, with $\sigma_{share} = 0.4$, was effective in generating a representative span of points between the nondominated boundary points.

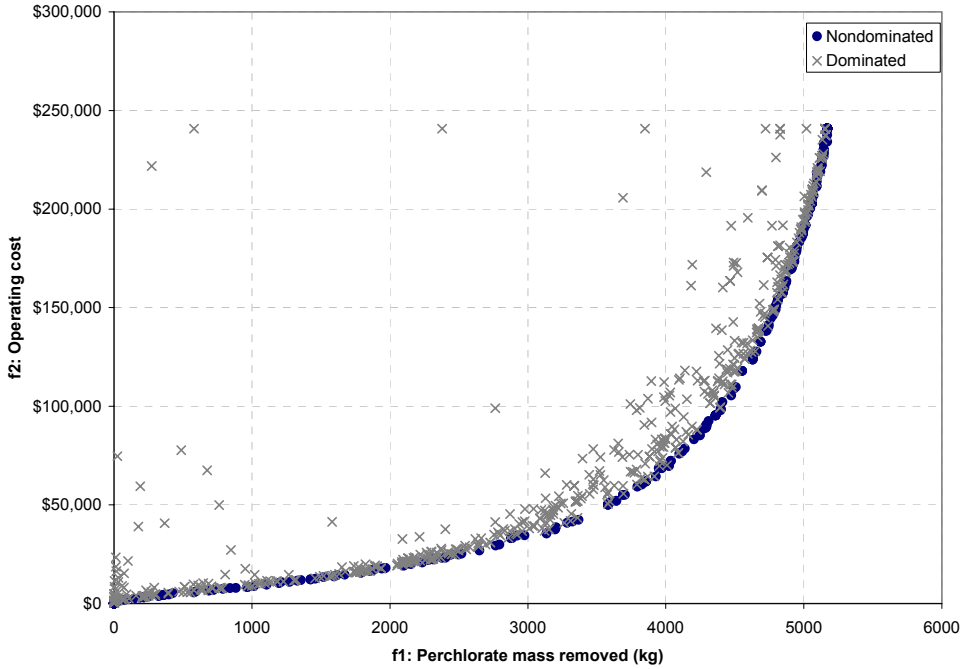

Figure 5. Run 1 est. Pareto front (t =300 days; Site 4 parameters).

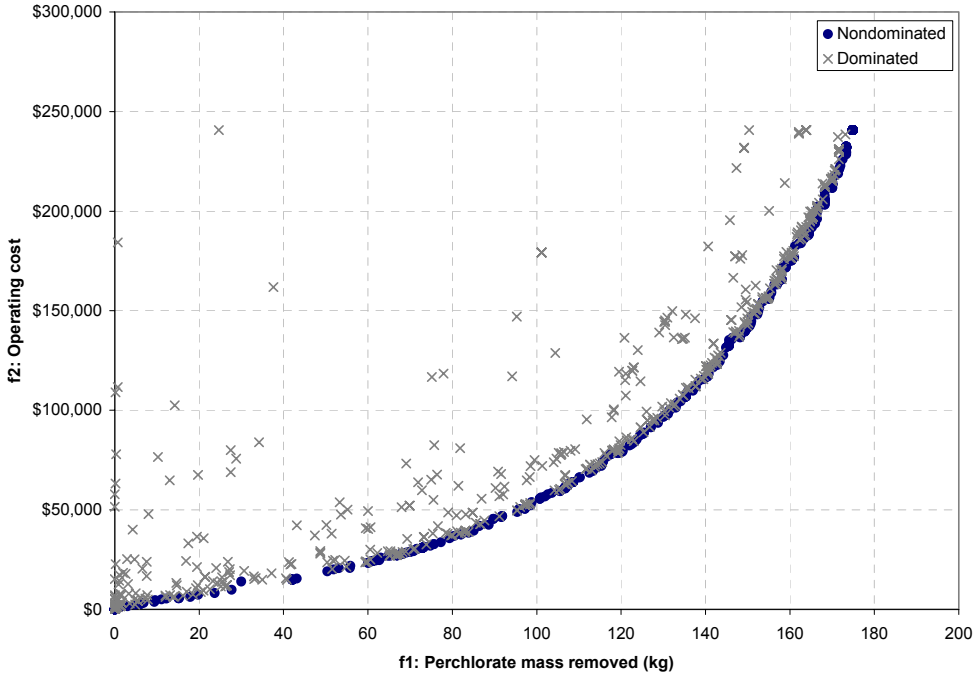

Figure 6. Run 2 est. Pareto front (t =300 days; Site 2 parameters).

Both nondominated fronts for Runs 1 and 2 exhibit a nonlinear relationship between f_1 and f_2, with df_2/df_1 increasing with increasing values of f_1. This indicates, as might be anticipated, that increments of perchlorate mass removal become increasingly expensive. Section 3.4 indicated that operating cost consisted of two parts: the cost of electron donor and the cost of operating the pumps. If Q assumes the value Q_{max}, then the cost of operating the pumps is maximized at about $780 for the 300-day period, which is a negligible component of total costs, which can be seen from Figures 5 and 6 to be in the tens of thousands of dollars for any mass removal much greater than zero. Therefore, high operating costs are essentially attributed to usage of electron donor alone.

One explanation for the increasing incremental costs of mass removal is that at high mass removal rates (which are needed to achieve high total mass removal) the perchlorate reduction reaction becomes limited, either by kinetics or by biomass. Thus, increasing donor is needed to achieve equivalent rates of perchlorate reduction, as perchlorate concentration increases. In the limit, the rate of perchlorate reduction is maximized and additional donor addition (resulting in increased cost) has no effect on the rate or extent of perchlorate reduction.

Runs 1 and 2 were for two different sites, with different hydraulic conductivities and initial ClO_4^- concentrations. Figure 7 plots PF_{known} for both Runs 1 and 2 on the same set of axes. Although PF_{known} for Runs 1 and 2 share the same range of operating cost values, nondominated points for Run 2 indicate considerably less mass-removal than those for Run 1. In fact, Figure 7 shows that, for the same operating cost of $240,771, Run 1 achieved a maximum mass-removal value of 5,170 kg of ClO_4^- destroyed compared to only 175 kg for Run 2. The large disparity in ClO_4^- removal performance is

almost certainly attributable to differences in hydrogeological properties. Hydraulic conductivity, which quantifies how easily water flows through the soil for a given hydraulic gradient, is about 3 times smaller in Site 2 than Site 4 (2.59 vs. 7.60 m/day); hydraulic gradient is also 10 times lower for Site 2 (0.001 vs. 0.010). The combination of these parameters results in a regional groundwater Darcy velocity for Site 2 that is ≈ 1/30 that of Site 4. This low Darcy velocity, in turn, causes higher interflow/recirculation between the two HFTWs for Site 2. Increased recirculation means that for a given pumping rate, there is less capture of upgradient contaminant by the treatment system, and less mass removal. Another potential reason for the mass-removal disparity between the two sites is the difference in initial ClO_4^- concentration: 330.0 mg/L for Run 1 (Site 4) versus 160.0 mg/L for Run 2 (Site 2). Clearly, contaminant mass removal is likely to be higher if higher concentrations of contaminant are present at the site.

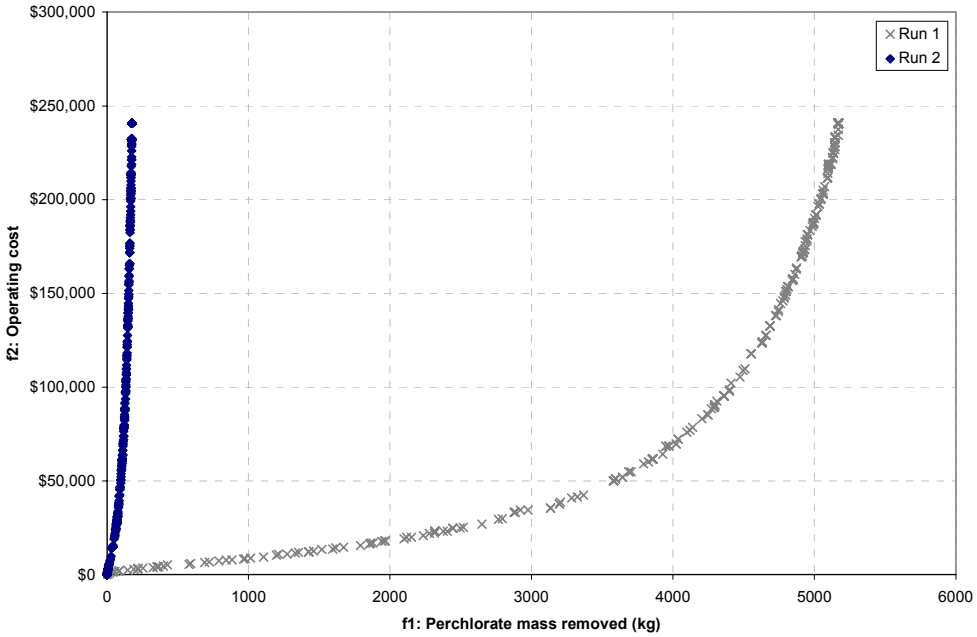

Figure 7. Runs 1 and 2 est. Pareto fronts (t =300 days).

The technology model also provided information about downgradient concentration ($[ClO_4^-]$) by comparing concentration values in all cells of column 20 of the discretized site model (Figure 3) and then outputting the *maximum* value. The purpose of observing this attribute was to assess the bioremediation technology's potential to attain hypothetical regulatory limits on downgradient contaminant levels.

Figure 8 shows the plot of maximum downgradient concentration versus ClO_4^- mass-removal for Run 1. The following observations can be made regarding this figure:

- In general, solutions (both nondominated and dominated) with higher mass removal tend to have lower concentration measurements, as would be expected. Note, however, that there are large individual variations within this general trend.
- Nondominated points with the lowest downgradient $[ClO_4^-]$ had very similar genotypes (*i.e.* decision variable values); Q, C_{in}, and p assumed values at or near Q_{max}, $C_{in,max}$, and p_{max}, respectively, indicating large mass per time of electron donor injected. Consequently, the objective function values associated with these points -tended to be relatively high: mass removal ≈ 5,170 kg and operating cost ≈ $241,000. Well spacing ($d$) was typically 25 meters. Downgradient $[ClO_4^-]$ for these particular nondominated solutions varied from 26 to 30 mg/L; greatly exceeding the state-specified action levels in the µg/L-range that were discussed in Section 2.1.
- Many dominated solutions, despite being inferior in terms of mass removal and cost, yielded lower ClO_4^- downgradient levels than their nondominated counterparts. Interestingly, the lowest concentration for Run 1 (24.1 mg/L) originates from a solution that is inferior to 326 other solutions.

Figure 9 shows the plot of maximum downgradient concentration versus ClO_4^- mass-removal for Run 2. The following observations apply to Figure 9:

- The plot of *all* points (both nondominated and dominated) reveals no discernible relationship between $[ClO_4^-]$ and mass removal.
- A chain of nondominated points with mass removal > 40.0 kg had relatively narrow range of downgradient $[ClO_4^-]$ values (8.4 – 8.7 mg/L); genotypes associated with $[ClO_4^-] \approx 8.4$ mg/L were nearly homogeneous; Q, C_{in}, and p had values at or near Q_{max}, $C_{in,max}$, and p_{max}, respectively, again indicating that mass of electron donor injected per time was large. Well separation (d) was typically 25 meters.
- Ironically, certain nondominated points associated with nearly-zero mass removal had *lower* $[ClO_4^-]$ values than other nondominated points with higher removals of ClO_4^- mass. These points had minimum values for Q as well as C_{in} and/or p minimized, indicating relatively low rates of donor mass injected per time. Well spacing (d) varied from 35 – 45 meters, and downgradient $[ClO_4^-]$ was $\approx 3\times10^{-4}$ mg/L, which complies with state-specified action levels mentioned Section 2.1. These low concentration measurements may be attributed to interflow (Section 2.2), which is a function of the design parameters (Q and d) and the regional groundwater Darcy velocity. Site 2 hydraulic conductivity is ≈ 1/3 that of Site 4, and Site 2 hydraulic gradient is 1/10 that of Site 4; this combination results in a regional groundwater Darcy velocity for Site 2 that is 30 times smaller than that of Site 4. Although the low Q for these solutions would tend to reduce interflow, the combination of low Darcy velocity and small well spacing ultimately

increases interflow. High interflow means that although very little contaminant mass is treated, the contaminated water that is treated ends up passing through the treatment wells multiple times, and downgradient contaminant concentrations would be low.

- Figure 9 shows a large number of dominated points that yielded lower ClO_4^- downgradient concentrations than other nondominated points. In fact, nondominated points with mass removal > 40.0 kg seem to establish an upper bound on measured concentration, with many dominated points lying below.

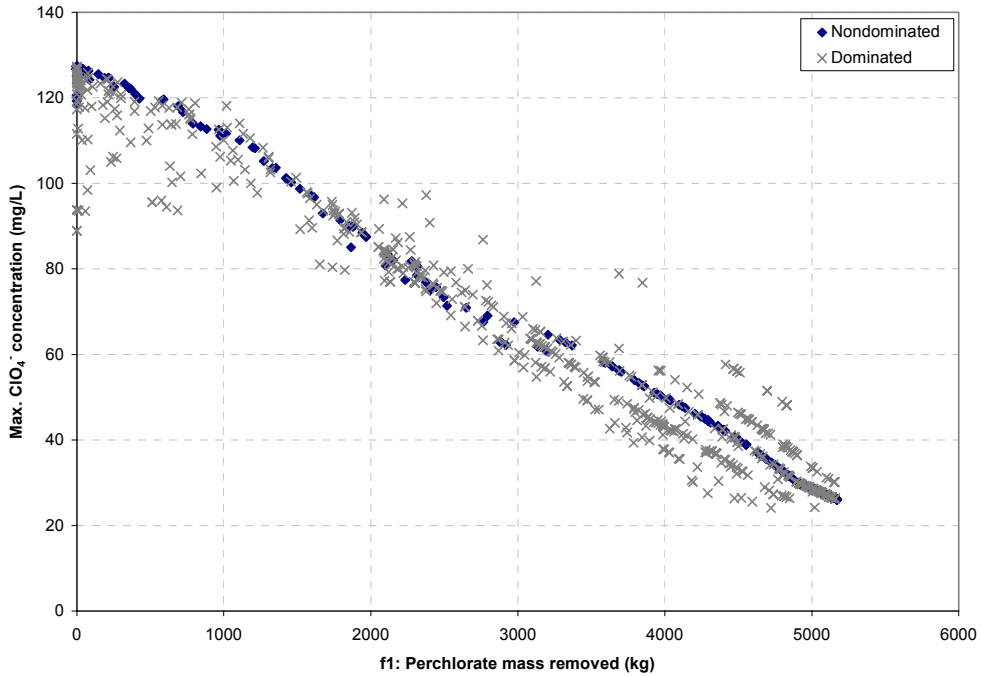

Figure 8. Run 1: maximum downgradient perchlorate conc. ($[ClO_4^-]$) vs. ClO_4^- mass removed.

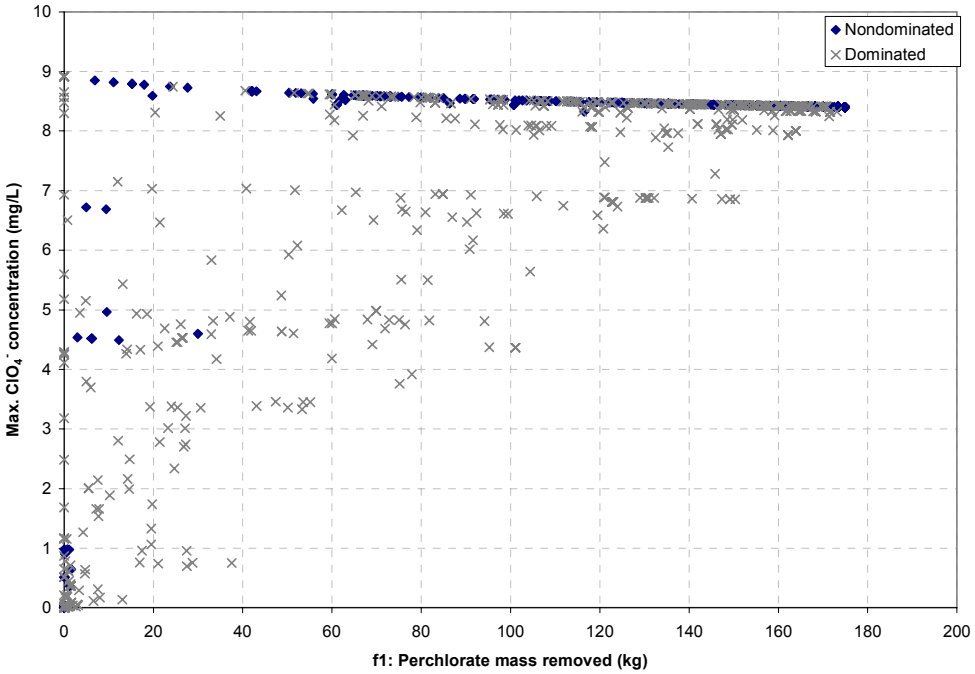

Figure 9. Run 2: maximum downgradient perchlorate conc. ([ClO_4^-]) vs. ClO_4^- mass removed.

4.3 RESULTS FOR 600-DAY TECHNOLOGY OPERATION

Figures 10 and 11 show the plots of PF_{known} for Runs 3 and 4, respectively, after 100 generations. These plots are very similar in shape to the respective 300-day runs (Figures 5 and 6), which is logical due to identical optimization parameters (except time). Upper boundary values for mass removal and operating cost are larger, of course, due to the longer time span. The same analysis used in section 4.1 can describe the nonlinear increase in incremental costs with mass removal that is seen here.

Figure 12 plots PF_{known} for Runs 3 and 4 on the same set of axes. Figure 12 reveals the same relationship that Figure 7 does: Site 4 parameters yield higher ClO_4^- mass removal than Site 2 parameters for the same range of operating cost for reasons mentioned previously with the 300-day simulations (different hydrogeolocial parameters and initial concentration).

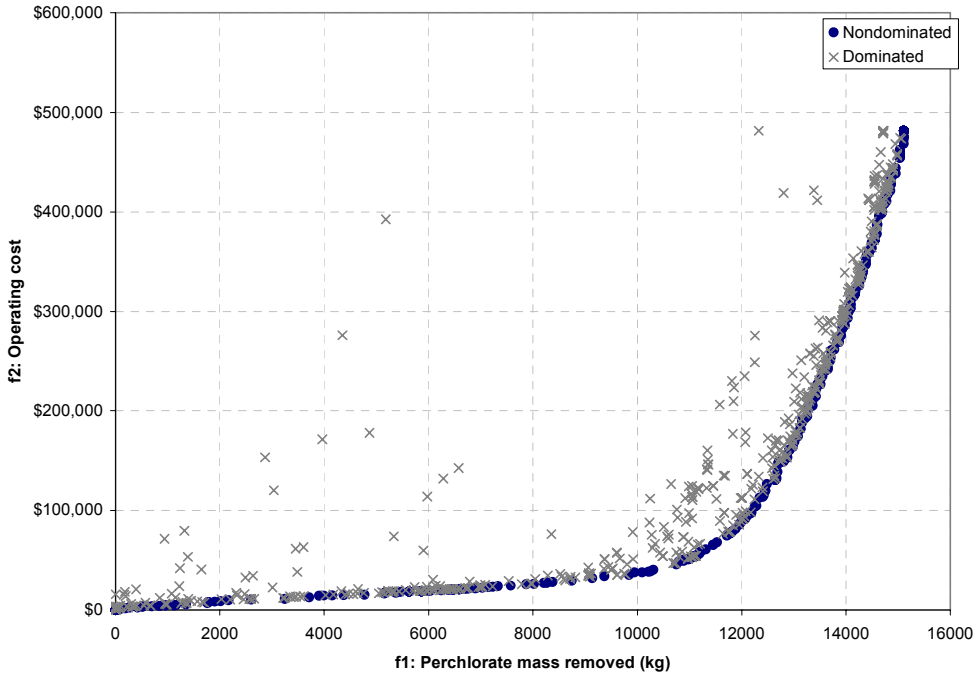

Figure 10. Run 3 est. Pareto front (t =600 days; Site 4 parameters).

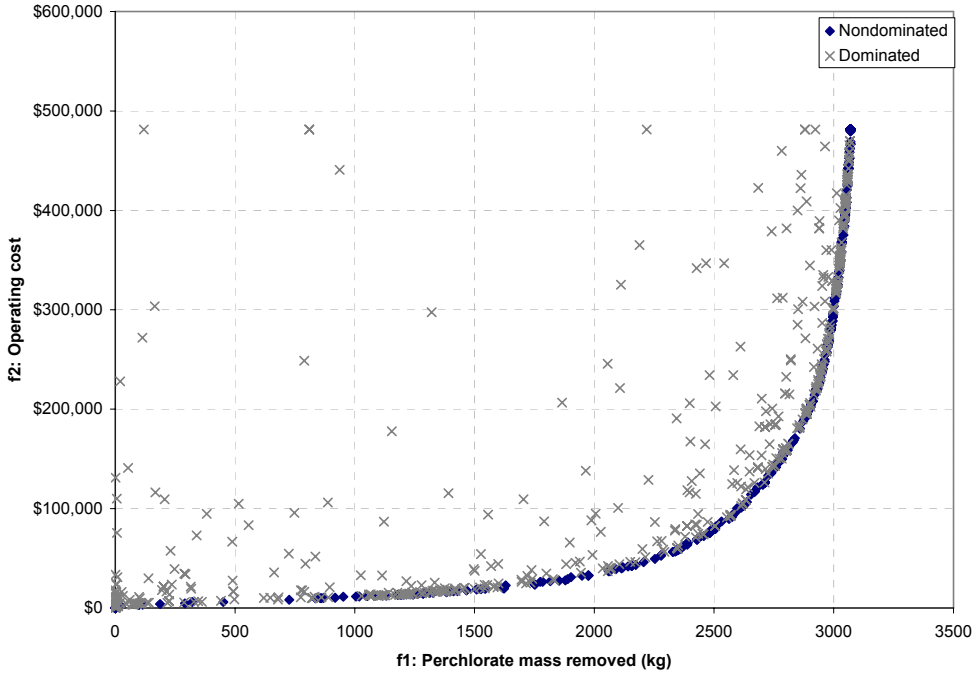

Figure 11. Run 4 est. Pareto front (t =600 days; Site 2 parameters).

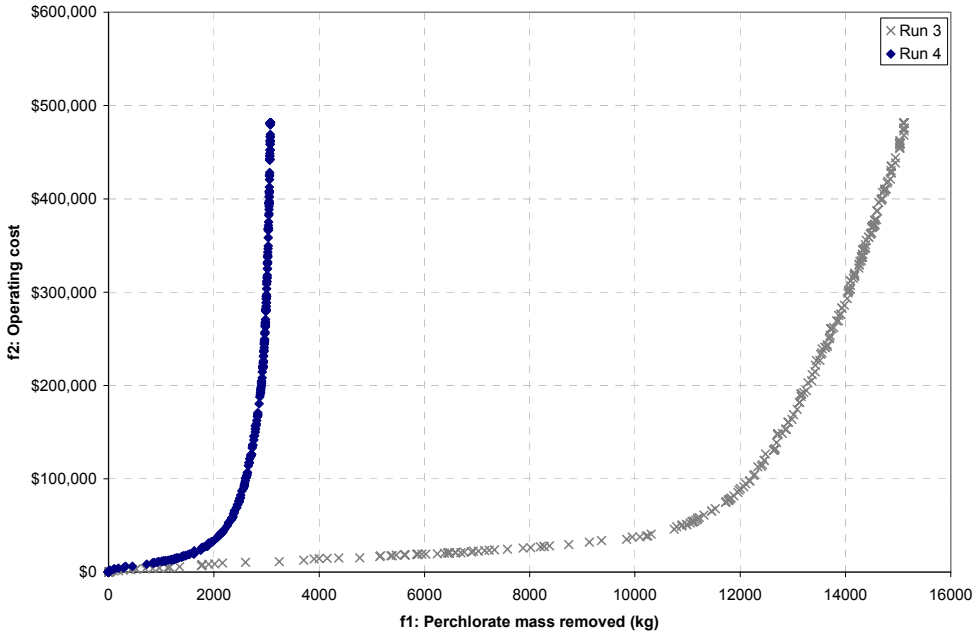

Figure 12. Runs 3 and 4 est. Pareto fronts (t =600 days).

Figure 13 plots maximum downgradient concentration versus ClO_4^- mass removal for Run 3 after 100 generations. The following observations can be made regarding Figure 13:

- Just like Run 1, solutions (both nondominated and dominated) with higher mass removal generally provide lower concentration measurements. Nondominated solutions appear to follow this trend better than the dominated solutions.
- 660 solutions had measured downgradient [ClO_4^-] that was *less* than the lowest value reported for Run 1 (24.1 mg/L); 283 of these solutions were nondominated. This seems to indicate that, for Site 4 parameters, downgradient ClO_4^- levels improve for longer treatment periods.
- Nondominated points with lowest downgradient [ClO_4^-] had very similar genotypes; Q, C_{in}, and p values at or near Q_{max}, $C_{in,max}$, and p_{max}, respectively, indicating large mass per time of electron donor injected and high operating cost

(≈$481,500). For these particular points, well spacing (*d*) was uniformly 25 meters, and downgradient [ClO_4^-] was ≈0.154 mg/L. Despite being an improvement over Run 1, this level still exceeds the state-specified action levels discussed in Section 2.1, which are in the µg/L range.

- Numerous dominated points, despite being inferior in terms of mass removal and cost, outperformed other nondominated points in achieving lower downgradient [ClO_4^-]. The lowest concentration for Run 3 (0.022 mg/L) originates from a solution inferior to 330 other solutions in terms of mass removal and cost.

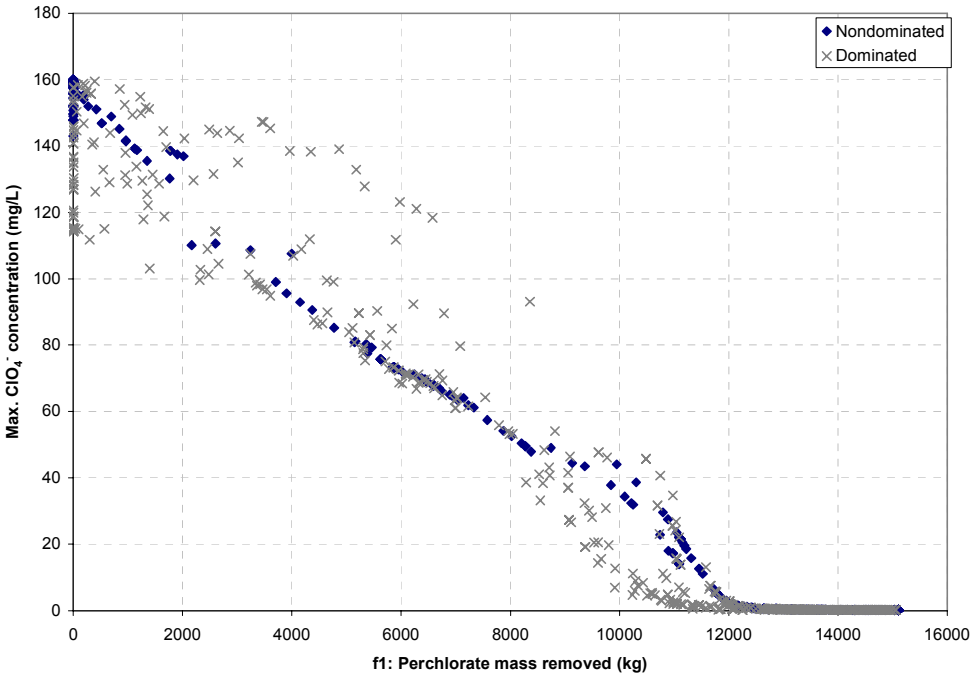

Figure 13. Run 3: maximum downgradient perchlorate conc. ([ClO_4^-]) vs. ClO_4^- mass removed.

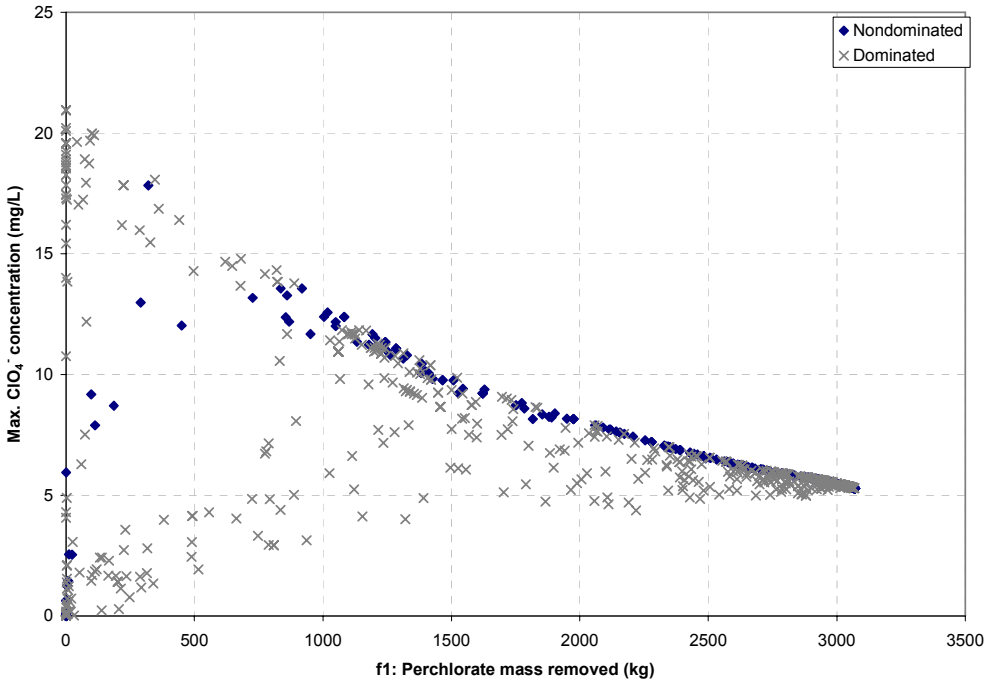

Figure 14. Run 4: maximum downgradient perchlorate conc. ($[ClO_4^-]$) vs. ClO_4^- mass removed.

Figure 14 plots maximum downgradient concentration versus ClO_4^- mass-removal for Run 2. The following observations apply to Figure 14:

- The plot of *all* points (both nondominated and dominated) reveals no discernible relationship between $[ClO_4^-]$ and mass removal.
- Nondominated solutions in the mass-removal range of >1,000 kg provided lower $[ClO_4^-]$ measurements as mass removal increased.
- Just like Run 2, Run 4 shows that certain nondominated points with negligible mass removal showed *lower* $[ClO_4^-]$ than other nondominated points with higher mass removal. These points had low Q values and one or both of C_{in} and p minimized, indicating small mass per time of electron donor injected. Well spacing (d) was minimized (3 meters), and downgradient $[ClO_4^-]$ was $\approx 9\times10^{-3}$

mg/L, which falls in the µg/L range of state-specified action levels discussed in Section 2.1. These low concentrations can also be attributed to high interflow (due to the low hydraulic conductivity and hydraulic gradient at the site) as previously explained for Run 2.

- A multitude of dominated points yielded better ClO_4^- downgradient concentrations than other nondominated points. In fact, nondominated points in the mass-removal range of >1,000 kg seem to establish an upper bound on measured concentration, with many dominated points lying below.

4.4 RESULTS SUMMARY

Runs 1, 2, 3, and 4 were performed to fulfill the objectives listed in Section 1.2. For each of the four runs, HK-MOGA estimated a Pareto front (Figures 5, 6, 10, and 11) that shows a nonlinear, increasing relationship between mass removal and operating cost. Figures 7 and 12 demonstrate that the bioremediation technology was less effective at removing ClO_4^- mass under Site 2 conditions than under Site 4 conditions. For Site 4 conditions, increasing the remediation time span from 300 to 600 days enabled the treatment technology to attain lower downgradient ClO_4^- concentrations; under Site 2 conditions, however, increasing the time span rendered no discernible improvement with respect to downgradient concentration. High mass removal of ClO_4^- is not necessarily coincident with lower ClO_4^- concentration, especially under Site 2 conditions.

5.0 CONCLUSIONS

5.1 SUMMARY

In this thesis effort, we developed and presented a method for optimizing applications of an innovative *in situ* bioremediation technology that uses HFTWs to remediate perchlorate- contaminated groundwater. The method involves coupling a multi-objective genetic algorithm with the technology model developed by Parr (2002). To meet the research goal and achieve the research objectives, it was necessary to use the technology model with appropriate parameters to simulate applications of the technology at representative sites, formulate a multi-objective problem, develop a multi-objective optimization algorithm that would be suitable to solve the problem by coupling with the technology model, and select appropriate HK-MOGA parameters. The method was applied to two sites having different hydrogeological conditions. HK-MOGA yielded system designs (flow rate, well spacing, injected nutrient concentration, and injection pulse duration) that provide valuable insights into the tradeoffs between 1) the technology's performance, defined by contaminant mass removal and 2) the operating costs incurred from implementing the technology.

The software used in this study was an adaptation of Garrett's (1999) GA code. In combination with Parr's (2002) technology model, HK-MOGA software can serve as a tool for both optimizing future applications of this innovative bioremediation technology, and helping us to better understand how HFTWs can be used in conjunction with *in situ*

biodegradation. This study contributes to efforts taken to resolve groundwater contamination problems caused by ClO_4^- releases across the United States.

5.2 CONCLUSIONS

- The multi-objective genetic algorithm (MOGA) developed in this study appeared useful for determining technology design parameters for *in situ* bioremediation of perchlorate using HFTWs to minimize cost (defined as operating cost) and maximize technology performance (defined as perchlorate mass removal). HK-MOGA determined various sets of design parameters (*Q, d, Cin, p*) that provided a decision maker with combinations of cost and mass removal that were "Pareto optimal", that is to say, nondominated by other potential solutions. This set of solutions allows a decision maker to select a system design based on the weighting of the relative importance of performance versus cost. One disadvantage of HK-MOGA is the need for relatively extensive computer resources (time and CPU power) to evaluate the technology model. Also, the selection of HK-MOGA parameters ($|Pop_0|$, $|MP|$, N, σ_{share}, p_m) was arbitrary, and based only on the experience and judgment of the investigator. It is unclear whether selection of a different set of parameters would result in a different outcome.
- Pareto fronts generated for all four simulations indicated that the incremental operating cost of the technology increases as the technology removes more perchlorate mass.

- For a contaminated site with relatively high conductivity and regional gradient, the choice of technology operating time affected the simulated concentrations of perchlorate downgradient of the treatment system. Extending the operating time from 300 to 600 days resulted in more nondominated solutions achieving maximum downgradient concentrations in the microgram-per-liter range.
- The technology's ability to remove perchlorate mass is poorly correlated with its ability to achieve diminished downgradient perchlorate concentrations, especially for a contaminated site with relatively low hydraulic conductivity and regional gradient. In other words, mass removal and diminished downgradient concentration are not redundant objectives. Therefore, decision makers must separately consider and weight each of these remediation goals when deciding on design parameters. It appears important to include downgradient perchlorate concentration as either an additional objective or a constraint when implementing a multi-objective optimization scheme.
- The ability of this technology to remediate perchlorate-contaminated groundwater is very difficult to ascertain for a variety of reasons. Results from the four simulations are based upon numerous simplifying assumptions about kinetic parameters and site properties, which may not be representative of field conditions. As Parr (2002) pointed out, literature values of kinetic parameters are "highly variable and sparse." The model requires validation with real-world data to properly judge the capability of *in situ* bioremediation technology.

5.3 RECOMMENDATIONS

Take advantage of the MOGA's power by formulating more general multi-objective problems. Due to time constraints, this study placed somewhat artificial (albeit realistic) limits on several of the design parameters that were being optimized. For instance, the study restricted the number of treatment wells to two, and also imposed restrictions on well location (e.g. the wells were spaced symmetrically about the site centerline and were at a specified distance downgradient of the source) and pumping rates (the two wells each pumped at the same rate). More generally, HK-MOGA could be applied where these decision variables could all be optimized.

To avoid over-constraining the problem, ClO_4^- concentration downgradient of the treatment system was not specified as a constraint. In reality, downgradient concentration would be an important parameter to use in defining technology effectiveness. Additionally, results of this study confirm that 1) reduction of contaminant mass and 2) reduction of downgradient contaminant concentration would *not* be redundant objectives for the *in situ* bioremediation technology. Future studies could implement downgradient concentration as a constraint or even as an additional objective function to be minimized.

Accuracy of model output could improve by modifying the perchlorate-contaminated site model (Figure 3). More numerous, smaller cells could improve accuracy of the technology model's spatially-dependent attributes like perchlorate mass removal and downgradient concentration, although this modification would be more computationally expensive.

Improve search performance by experimenting with the HK-MOGA's parameters or adopting a different MOGA. There was no theoretical basis for selecting values for $|Pop_0|$, $|MP|$, N, σ_{share}, and σ_{share}; factors such as off-line experimentation with HK-MOGA, literature values, and resource constraints guided the author in assigning values to these parameters. Additional simulations could provide an empirical means to determine the optimal blend of parameter values that improve the search for Pareto optimal solutions.

Chapter 2 described several MOGAs, such as NPGA, NSGA, NSGA-II, and SPEA. For this study, NPGA was selected as the most appropriate due to its ease of implementation and its success in solving a multi-objective groundwater remediation problem with objectives similar to the ones in this study (Erickson *et al*., 2001). Newer MOGAs, like NSGA-II, and SPEA, have an advantage over NPGA and NSGA because their fitness sharing methods do not require user-specified parameters. However, as can be seen from the literature, research in this area is advancing rapidly, and in a future study a more efficient algorithm may be available for application to this problem.

Validate the model with field data. A field evaluation of *in situ* bioremediation of TCE using HFTWs has already been performed at the Edwards AFB, Site 19 (McCarty *et al*., 1998). A similar field evaluation is scheduled to begin this year to study a pilot-scale system to treat perchlorate-contaminated groundwater. Results and analysis of this evaluation will offer the opportunity to ascertain kinetic parameters for use in technology

design. The results obtained from operation of the pilot-scale, *in situ* bioremediation system could also provide data necessary to validate Parr's (2002) technology model.

APPENDIX A: TECHNOLOGY MODEL EQUATIONS

The Parr (2002) technology model is a set of partial differential equations representing flow and transport (equations A.1 – A.4), biological reactions (equations A.5 – A.8), and biomass growth (equation A.12) in a subsurface system with microorganisms utilizing an electron donor (acetate) to reduce three electron acceptors (ClO_4^-, oxygen, and nitrate). This section provides further detail on the equations that are the technology model.

FLOW AND TRANSPORT MODEL (PARR, 2002)

The Parr (2002) technology model solves four separate, 3-dimensional advection/dispersion equations (A.1 – A.4) that represent transport of the electron donor (acetate CH_3COO^-) and three electron acceptors (oxygen, nitrate, and ClO_4^-), respectively. The left side of equation A.1 includes a retardation factor (R) that accounts for sorption of the electron donor; sorption is assumed to be an equilibrium process that is both linear and reversible. On the other hand, equations A.2 – A.4 use $R=1$, as the electron acceptors (O_2, NO_3^-, ClO_4^-) are assumed to be non-sorbing. The right-hand sides of equations A.1-A.4 include dispersion terms ($D\nabla^2 C$) and advection terms ($v\nabla C$) for the electron donor and acceptors. The rightmost terms in equations A.1 – A.4 are source/sink terms that represent production/consumption rates (r) due to microbial redox reactions.

$$\frac{\partial C^{don}}{\partial t} \cdot R = D \cdot \nabla^2 C^{don} - v \cdot \nabla C^{don} + r_{donor} \qquad \text{(A.1)}$$

$$\frac{\partial C^{oxy}}{\partial t} = D \cdot \nabla^2 C^{oxy} - v \cdot \nabla C^{oxy} + r_{oxy} \qquad \text{(A.2)}$$

$$\frac{\partial C^{nit}}{\partial t} = D \cdot \nabla^2 C^{nit} - v \cdot \nabla C^{nitn} + r_{nit} \qquad \text{(A.3)}$$

$$\frac{\partial C^{per}}{\partial t} = D \cdot \nabla^2 C^{per} - v \cdot \nabla C^{per} + r_{per} \qquad \text{(A.4)}$$

where

C^{don} = concentration of the electron donor (acetate) (mg/L)

C^{oxy} = concentration of oxygen (an electron acceptor) (mg/L)

C^{nit} = concentration of nitrate (an electron acceptor) (mg/L)

C^{per} = concentration of ClO_4^- (an electron acceptor) (mg/L)

t = time (days).

D = dispersion (m^2/day);

v = average linear velocity of groundwater (m/day)

R = retardation factor; accounts for sorption of the electron donor

r_{donor} = rate of electron donor consumption (mg donor/L/day)

r_{oxy} = rate of oxygen consumption (mg oxygen/L/day)

r_{nit} = rate of nitrate consumption (mg nitrate/L/day)

r_{per} = rate of ClO_4^- consumption (mg ClO_4^-/L/day)

BIOLOGICAL TREATMENT SUBMODEL (PARR, 2002)

Equations A.5 – A.8 and A.12 comprise the biological treatment submodel. As mentioned previously, the rightmost terms in equations A.1 – A.4 are production/consumption rates due to microbial redox reactions; these terms are formulated based on a dual-Monod, multi-electron acceptor biodegradation model proposed by Envirogen (Parr, 2002). These reaction terms are defined as follows (note that the negative sign indicates consumption):

$$r_{donor} = \frac{dC^{don}}{dt} = -X \cdot (r_{don,oxy} + r_{don,nit} + r_{don,per}) \qquad \text{(A.5)}$$

$$r_{oxy} = \frac{dC^{oxy}}{dt} = -X \cdot F_{oxy} \cdot k_{\max} \left[\frac{C^{don}}{K_S^{don} + C^{don}} \right] \cdot \left[\frac{C^{oxy}}{K_S^{oxy} + C^{oxy}} \right] \qquad \text{(A.6)}$$

$$r_{nit} = \frac{dC^{nit}}{dt} = -X \cdot F_{nit} \cdot k_{\max} \left[\frac{C^{don}}{K_S^{don} + C^{don}} \right] \cdot \left[\frac{C^{nit}}{K_S^{nit} + C^{nit}} \right] \cdot \left[\frac{K_i^{oxy}}{K_i^{oxy} + C^{oxy}} \right] \qquad \text{(A.7)}$$

$$r_{per} = \frac{dC^{per}}{dt} = -X \cdot F_{per} \cdot k_{\max} \left[\frac{C^{don}}{K_S^{don} + C^{don}} \right] \cdot \left[\frac{C^{per}}{K_S^{per} + C^{per}} \right] \cdot \left[\frac{K_i^{oxy}}{K_i^{oxy} + C^{oxy}} \right] \cdot \left[\frac{K_i^{nit}}{K_i^{nit} + C^{nit}} \right] \qquad \text{(A.8)}$$

where

r_{donor} = rate of electron donor consumption (mg donor/L/day)

$r_{don,oxy}$ = specific rate of electron donor consumption using oxygen as an electron acceptor (mg donor/mg biomass/day); see equation A.9

$r_{don,nit}$ = specific rate of electron donor consumption using nitrate as an electron acceptor (mg donor/mg biomass/day); see equation A.10

$r_{don,per}$ = specific rate of electron donor consumption using ClO_4^- as an electron acceptor (mg donor/mg biomass/day); see equation A.11

r_{oxy} = rate of oxygen consumption (mg oxygen/L/day)

r_{nit} = rate of nitrate consumption (mg nitrate/L/day)

r_{per} = rate of ClO_4^- consumption (mg ClO_4^-/L/day)

X = concentration of active microorganisms (mg/L)

F_{oxy} = stoichiometric coefficient for the donor (acetate)-oxygen reaction (mg oxygen/mg donor) where the stoichiometric coefficient accounts for the electron acceptor requirement for biomass production based on the following stoichiometry ($C_5H_9NO_3$ represents the chemical formula for biomass) (Envirogen, 2002a):

$$O_2 + 0.64\ CH_3COOH + 0.056\ NH_4OH \rightarrow 0.056\ C_5H_9NO_3 + 0.168\ H_20 + 1.0\ H_2CO_3$$

F_{nit} = stoichiometric coefficient for the donor (acetate)-nitrate reaction (mg nitrate/mg donor) where the coefficient accounts for the electron acceptor requirement for biomass production (Envirogen, 2002a):

$$NO_3^- + 0.786\ CH_3COOH \leftrightarrow 0.056\ C_5H_9NO_3 + 0.472N_2 + 0.528\ H_20 + 0.292\ H_2CO_3 + HCO_3^-$$

F_{per} = stoichiometric coefficient for the donor (acetate)-ClO_4^- reaction (mg ClO_4^-/mg donor) where the coefficient accounts for the electron acceptor requirement for biomass production (Envirogen, 2002a):

$$ClO_4^- + 1.141\ CH_3COOH + 0.056NH_4OH \leftrightarrow 0.056\ C_5H_9NO_3 + Cl^- + 2.002\ H_2CO_3 + 0.164\ H_20$$

k_{max} = maximum specific rate of substrate utilization (mg donor/mg biomass/day)

K_S^{oxy} = half saturation concentration when oxygen (an electron acceptor) concentration is varied and limiting (mg/L)

K_S^{nit} = half saturation concentration when nitrate (an electron acceptor) concentration is varied and limiting (mg/L)

K_S^{per} = half saturation concentration when ClO_4^- (an electron acceptor) concentration is varied and limiting (mg/L)

K_i^{oxy} = oxygen inhibition coefficient (mg/L)

K_i^{nit} = nitrate inhibition coefficient (mg/L)

K_S^{don} = donor half saturation concentration (mg donor/L)

Equations A.7 and A.8 have inhibition coefficients (K_i) to account for competitive effects among electron acceptors. Equation A.7 includes an oxygen inhibition coefficient (K_i^{oxy}) because the presence of oxygen inhibits microbial reduction of nitrate. If oxygen is absent ($C^{oxy} = 0$), then K_i^{oxy} has no influence on r_{nit} because the rightmost fraction of equation A.7 becomes 1. Similarly, equation A.8 includes both oxygen and nitrate inhibition coefficients (K_i^{oxy} and K_i^{nit}) because the presence of either oxygen or nitrate inhibits microbial reduction of ClO_4^-. Parr (2002) cites laboratory results that demonstrate how oxygen and nitrate inhibit microbial reduction of less preferable electron acceptors, like ClO_4^-.

Parr (2002) assumed that inhibition coefficients are equal to their respective half saturation concentrations (i.e. $K_S^{oxy} = K_i^{oxy}$ and $K_S^{nit} = K_i^{nit}$). Also, equation A.5 contains the terms $r_{don,oxy}$, $r_{don,nit}$, and $r_{don,per}$, which are defined as follows:

$$r_{don,oxy} = k_{\max}^{don/oxy}\left[\frac{C^{don}}{K_S^{don/oxy} + C^{don}}\right]\cdot\left[\frac{C^{oxy}}{K_S^{oxy} + C^{oxy}}\right] \qquad \text{(A.9)}$$

$$r_{don,nit} = k_{\max}^{don/nit}\left[\frac{C^{don}}{K_S^{don/nit} + C^{don}}\right]\cdot\left[\frac{C^{nit}}{K_S^{nit} + C^{nit}}\right]\cdot\left[\frac{K_i^{oxy}}{K_i^{oxy} + C^{oxy}}\right] \qquad \text{(A.10)}$$

$$r_{don,per} = k_{\max}^{don/per}\left[\frac{C^{don}}{K_S^{don/per} + C^{don}}\right]\cdot\left[\frac{C^{per}}{K_S^{per} + C^{per}}\right]\cdot\left[\frac{K_i^{oxy}}{K_i^{oxy} + C^{oxy}}\right]\cdot\left[\frac{K_i^{nit}}{K_i^{nit} + C^{nit}}\right] \qquad \text{(A.11)}$$

where

$k_{max}^{don/oxy}$ = maximum specific rate of substrate utilization in the presence of oxygen when donor concentration is varied and limiting (mg donor/mg biomass/day)

$k_{max}^{don/nit}$ = maximum growth rate of substrate utilization in the presence of nitrate when donor concentration is varied and limiting (mg donor/mg biomass/day)

$k_{max}^{don/per}$ = maximum specific rate of substrate utilization in the presence of ClO_4^- when donor concentration is varied and limiting (mg donor/mg biomass/day)

$K_S^{don/oxy}$ = half saturation concentration of the electron donor in the presence of oxygen when donor (acetate) concentration is varied and limiting (mg donor/L)

$K_S^{don/nit}$ = half saturation concentration of the electron donor in the presence of nitrate when donor (acetate) concentration is varied and limiting (mg donor/L)

$K_S^{don/per}$ = half saturation concentration of the electron donor in the presence of ClO_4^- when donor (acetate) concentration is varied and limiting (mg donor/L)

The microbial growth/decay equation of the technology model is

$$\frac{dX}{dt} = X \cdot \left[Y_{biomass} \cdot (r_{don,oxy} + r_{don,nit} + r_{don,per}) - b \right]; \; X > X_{\min} \qquad \text{(A.12)}$$

$$\frac{dX}{dt} = 0; X \le X_{\min}$$

where

X_{min} = minimum biomass concentration (mg/L)

$Y_{biomass}$ = the biomass yield per mass of donor consumed (mg biomass/mg electron donor)

b = biomass decay rate (day^{-1})

Equation A.12 assumes that biomass concentration will never decrease below some minimum (X_{min}).

APPENDIX B: DERIVATION OF ENERGY CONSTANT

In this study, we assume that each HFTW uses a static mixer to blend the substrate (acetate) with water. It is further assumed that pumping costs depend primarily on the energy necessary to overcome head losses from the static mixer.

We assume that the static mixers will be installed in very smooth pipes of diameter D = 1.25 inches (0.0318 m) and length L = 4.0 m, which is the distance between the upper and lower screens of each HFTW. Also, we assume that water has a kinematic viscosity ν = 1.141 m^2/sec @ 15° C. Dividing flow rate Q by the pipe's cross-sectional area $A = \pi D^2/4$ yields velocity V. The Reynolds number can be calculated as follows:

$$\mathrm{Re} = VD/\nu \qquad \text{(B.1)}$$

Recall from Section 3.6 that the minimum and maximum values for Q are 10 and 150 m^3/day, which correspond to Reynolds numbers of 4,060. and 60,900, respectively. Hence, flow is clearly turbulent (Re > 2,000) for all possible values of Q.

The Blasius equation can be used to obtain the friction factor f for 3,000 < Re < 100,000 (Daugherty & Franzini, 1965:212):

$$f = 0.316/(\mathrm{Re}^{0.25}) \qquad \text{(B.2)}$$

Knowing f enables computation of the empty-pipe head loss h_L via the Darcy-Weisbach equation (Mays, 2001:419):

$$h_L = 8fLQ^2/(\pi^2\, g\, D^5) \quad \text{(B.3)}$$

Cleveland Eastern Mixers supplied the following equation for computing the flow coefficient (Cf) for Re > 1000:

$$Cf = -15.9 + 8.41 \ln(Re) \qquad (B.4)$$

The flow coefficient is used to account for the headloss through the static mixer elements ($h_{L,static}$), using equation B.5 below:

$$h_{L,static} = Cf \cdot h_L \qquad (B.5)$$

Finally, given that the unit weight of water is γ [units of force-per-m^3], the energy-per-m^3 of water required to overcome $h_{L,static}$ can be written as

$$E = \gamma \, h_{L,static} \qquad (B.6)$$

BIBLIOGRAPHY

Amadei, G.A., and J.E. Earley. "Effect of Some Macrocyclic Ligands on the Rate of Reduction of Perchlorate Ion by Titanium(III)," *Croatia Chemica Acta, 74*(3): 601-606 (2001).

Beasley, D., D.R. Bull, and R.R. Martin. "An Overview of Genetic Algorithms: Part 1, Fundamentals," *University Computing*, *15*: 58-69 (1993).

California Environmental Protection Agency (CEPA), Office of Environmental Health Hazard Assessment (OEHHA). *DRAFT: Public Health Goal for Perchlorate in Drinking Water*, March 2002.

Christ, J. A., *A Modeling Study for the Implementation of In Situ Cometabolic Bioremediation of Trichloroethylene-Contaminated Groundwater*. MS Thesis, AFIT/GEE/ENV/97D-03. School of Engineering and Environmental Management, Air Force Institute of Technology, (AU), Wright-Patterson AFB OH, December 1997.

Christ, J. A., M.N. Goltz, and J. Huang. "Development and Application of an Analytical Model to Aid Design and Implementation of In Situ Remediation Technologies," *Journal of Contaminant Hydrology*, *37*(3): 295-317, 1999.

Coello Coello, A. C., D.A. Van Veldhuizen, and G.B. Lamont. *Evolutionary Algorithms for Solving Multi-Objective Problems*, New York: Kluwer Academic/Plenum Publishers, 2002.

Coley, David A. *Introduction to Genetic Algorithms for Scientists and Engineers*. River Edge NJ: World Scientific Publishing Company, Inc., 1999.

Daugherty, R. L., and J. B. Franzini. *Fluid Mechanics with Engineering Applications*. New York: McGraw-Hill Book Company, 1965.

Deb, K., A. Pratap, S. Agarwal, and T. Meyarivan. "A Fast and Elitist Multi-Objective Genetic Algorithm: NSGA-II," *IEEE Transactions on Evolutionary Computation*, 6(2):182-197, April 2002.

Domenico, P.A., and F.W. Schwartz. *Physical and Chemical Hydrogeology*, New York: John Wiley & Sons, Inc., 1998.

Earley, J. E. Sr., D.C. Tofan, and G.A. Amadei. "Reduction of Perchlorate Ion by Titanous Ions in Ethanolic Solution," *Perchlorate in the Environment.* Ed. Urbansky, E. T.; Kluwer Academic/Plenum Publishers, New York, 2000.

Environmental Protection Agency (EPA). *Region 9 Perchlorate Update*. June 1999.

Environmental Security Technology Certification Program (ESTCP). *In Situ* Bioremediation of Perchlorate in Groundwater. http://www.estcp.org/projects/cleanup/. 25 November 2002.

Espenson, J.H. "The Problem and Perversity of Perchlorate," *Perchlorate in the Environment.* Ed. Urbansky, E. T.; Kluwer Academic/Plenum Publishers, New York, 2000.

Erickson, M., A. Mayer, and J. Horn. "Multi-objective Optimal Design of Groundwater Remediation Systems: Application of the Niche Pareto Genetic Algorithm," *Advances in Water Resources* 25: 51-65, 2002.

Federal Register. Vol. 67, No. 1. Wednesday, January 2, 2002. Notices.

Ferland, D. R., *In Situ Treatment of Chlorinated Ethene-Contaminated Groundwater Using Horizontal Flow Treatment Wells*. MS Thesis, AFIT/GEE/ENV/00M-05, 2000. School of Engineering and Environmental Management, Air Force Institute of Technology, (AU), Wright-Patterson AFB OH, December 2000.

Ferland, D.R., and M.N. Goltz. "Contain and Destroy: Designing a Horizontal Flow Treatment Well System to Remediate Groundwater Contamination," *The Military Engineer*, *611*:45-47 (March-April 2001).

Flowers, T.C., and J.R. Hunt. "Long-Term Release of Perchlorate as a Potential Source Of Groundwater Contamination," *Perchlorate in the Environment*. Ed. Urbansky, E. T.; Kluwer Academic/Plenum Publishers, New York, 2000.

Fonseca, C.M., and P.J. Fleming. "Genetic Algorithms for Multi-objective Optimization: Formulation, Discussion and Generalization," *Proceedings of the 5th ICGA*, 416-423, 1993.

Fonseca, C.M., and P.J. Fleming. "An Overview of Evolutionary Algorithms in Multiobjective Optimization," *Evolutionary Computation* 3(1), 1-16, 1995.

Gandhi, R.K., G.D. Hopkins, M.N. Goltz, S.M. Gorelick and P.L. McCarty. "Full-Scale Demonstration of *In Situ* Cometabolic Biodegradation of Trichloroethylene in Groundwater, 1: Dynamics of A Recirculating Well System," *Water Resources Research*, *38*(4): 10.1029/2001WR000379, 2002a.

Gandhi, R.K., G.D. Hopkins, M.N. Goltz, S.M. Gorelick and P.L. McCarty. "Full-Scale Demonstration of *In Situ* Cometabolic Biodegradation of Trichloroethylene in Groundwater, 2: Comprehensive Analysis Of Field Data Using Reactive Transport Modeling," *Water Resources Research*, *38*(4): 10.1029/ 2001WR000380, 2002b.

Garrett, C.A., *Optimization of In Situ Aerobic Cometabolic Bioremediation of Trichloroehylene-Contaminated Groundwater Using A Parallel Genetic Algorithm*. MS thesis, AFIT/GEE/ENV/99M-02. School of Engineering and Environmental

Management, Air Force Institute of Technology (AU), Wright-Patterson AFB OH, December 1999.

Goldberg, David E. *Genetic Algorithms in Search, Optimization, and Learning*. Reading MA: Addison-Wesley, 1989.

Goldberg, D. E., and J. Richardson. "Genetic Algorithms with Sharing for Multimodal Function Optimization," *Proc. 2nd Int. Conf. on Genetic Algorithms*, pp 41-49, Cambridge, MA, 1987.

Greene, M. R. and M. P. Pitre. "Treatment of Groundwater Containing Perchlorate Using Biological Fluidized Bed Reactors with GAC or Sand Media," *Perchlorate in the Environment.* Ed. Urbansky, E. T.; Kluwer Academic/Plenum Publishers, New York, 2000.

Gurol, M.D., and K. Kim. "Investigation of Perchlorate Removal in Drinking Water Sources by Chemical Methods," *Perchlorate in the Environment.* Ed. Urbansky, E. T.; Kluwer Academic/Plenum Publishers, New York, 2000.

Harbaugh, A.W. and M.G. McDonald. User's documentation for MODFLOW-96, and update to the US Geological Survey modular finite-difference groundwater flow model; US Geological Survey Open-File Report 1996, 96-485, 56p.

Hatzinger, P.B., M.R. Greene, S. Frisch, A.P. Togna, J. Manning, and W.J. Guarini. "Biological Treatment of Perchlorate-Contaminated Groundwater Using Fluidized Bed Reactors," *2nd International Conference on Remediation of Chlorinated and Recalcitrant Compounds*, Monterey CA, May 22-25, 2000.

Holland, John H. *Adaptation in Natural and Artificial Systems: an Introductory Analysis with Applications to Biology, Control, and Artificial Intelligence*. Cambridge MA: MIT Press, 1992.

Horn, J., N. Nafpliotis, and D.E. Goldberg. "A Niched Pareto Genetic Algorithm for Multiobjective Optimization," *Proceedings of the 1st ICEC*, 82-87, 1994.

Huang, J. and M. N. Goltz. "A Model of *In Situ* Bioremediation which Includes the Effect of Rate Limited Sorption and Bioavailability." *Proceedings of the 1998 Conference on Hazardous Waste Research,* pp 297-295, Snow Bird UT, 19-21 May 1998.

Logan, B. E. "A Review of Chlorate- and Perchlorate-Respiring Microorganisms," *Bioremediation Journal*, *2*(2): 69-79, 1998.

Logan, B. E. "Assessing the Outlook for Perchlorate Remediation," *Environmental Science and Technology*, 35(23): 482A-487A, 2001.

Mays, Larry W. *Water Resources Engineering*. New York: John Wiley & Sons, Inc., 2001.

McCarty, P. L., M. N. Goltz, G. D. Hopkins, M. E. Dolan, J. P. Allan, B. T. Kawakami, and T. J. Carrothers. "Full-Scale Evaluation of In Situ Cometabolic Degradation of Trichloroethylene in Groundwater through Toluene Injection," *Environmental Science and Technology*, *32*(1): 88-100, 1998.

McMaster, M.L., E.E. Cox, S.L. Neville, and L.T. Bonsack. "Successful Field Demonstration of In Situ Bioremediation of Perchlorate in Groundwater," In: Bioremediation of Inorganic Compounds, A. Leeson *et al*. eds. *Proceedings of the Sixth International In Situ and On-Site Bioremediation Symposium*, June 4-7, San Diego, CA, 6(9): 297-302, 2001.

Michalewicz, Zbigniew. *Genetic Algorithms + Data Structures = Evolution Programs*. USA: Springer, 1994.

Mitchell, Melanie. *An Introduction to Genetic Algorithms*. Cambridge, MA: MIT Press, 1996.

Parr, J.C. *Application of Horizontal Flow Treatment Wells for In Situ Treatment of Perchlorate Contaminated Groundwater*. MS thesis, AFIT/GEE/ENV/02M-08. School of Engineering and Environmental Management, Air Force Institute of Technology (AU), Wright-Patterson AFB OH, March 2002.

Parsons, *Groundwater Circulation Well Technology Evaluation at Facility 1381, Cape Canaveral Air Station, Florida, Technical Summary Report*, Prepared for Air Force Center for Environmental Excellence, April 2002.

Rikken, G.B., A.G.M. Kroon, and C.G. van Ginkel. "Transformation of (Per)chlorate into Chloride by a Newly Isolated Bacterium: Reduction and Dismutation," *Applied Microbiological Biotechnology*, 45: 420-426, 1996.

Ringuest, Jeffrey L. *Multiobjective Optimization: Behavioral and Computational Considerations*, Boston: Kluwer Academic Publishers, 1992.

Sawaragi, Y., H. Nakayama, and T. Tanino. *Theory of Multiobjective Optimization*, Orlando FL: Academic Press, Inc., 1985.

Srinivas, N., and K. Deb. "Multiobjective Optimization Using Nondominated Sorting in Genetic Algorithms," *Evolutionary Computation* 2(3), 221-248, 1994.

Stoppel, C. M., *A Model for Palladium Catalyzed Destruction of Chlorinated Ethene Contaminated Groundwater.* MS Thesis, AFIT/GEE/ENV/01M-21, 2001. School of Engineering and Environmental Management, Air Force Institute of Technology, (AU), Wright-Patterson AFB OH, 2001.

Stoppel, C. M. and M. N. Goltz, "Modeling Pd-Catalyzed Destruction of Chlorinated Ethenes in Groundwater, *ASCE Journal of Environmental Engineering*, 129(2):147-154, 2002.

United States Department of Energy (USDOE), Energy Information Administration. Table 1. U.S. Average Monthly Bill By Sector, Census Division and State, 2000 COMMERCIAL. http://www.eia.doe.gov/cneaf/electricity/esr/esrt01p2.html. 26 December 2002.

Urbansky, E. T. "Perchlorate Chemistry: Implications for Analysis and Remediation," *Bioremediation Journal*, 2: 81-95, 1998.

Urbansky, E.T. and M.R. Schock. "Issues in Managing the Risks Associated with Perchlorate in Drinking Water," Journal *of Environmental Management*. *56*: 79-95, 1999.

Van Veldhuizen, David A. *Multiobjective Evolutionary Algorithms: Classifications, Analyses, and New Innovations*. Air Force Institute of Technology (AU), Wright-Patterson AFB OH, June 1999.

Van Veldhuizen, D.A., and G.B. Lamont. "Multiobjective Evolutionary Algorithms: Analyzing the State of the Art," *Evolutionary Computation 8*(2):125-147, Summer 2000.

Whitley, Darrell. "A Genetic Algorithm Tutorial," *Statistics and Computing*, *4*(2): 65-85 June 1994.

Wu, J., R.F. Unz, H. Zhang, and B.E. Logan. "Persistence of Perchlorate and the Relative Numbers of Perchlorate- and Chlorate-Respiring Microorganisms in Natural Waters, Soils, and Wastewater," *Bioremediation Journal*, *5*(2): 119-130, 2001.

Zitzler, E., and L. Thiele. "Multiobjective Evolutionary Algorithms: a Comparative Case Study and the Strength Pareto Approach," *IEEE Transactions on Evolutionary Computation*, 3(4):257-271, November 1998.

Zydallis, J. B., D. A. Van Veldhuizen, and G. B. Lamont. "A Statistical Comparison of Multiobjective Evolutionary Algorithms Including the MOMGA-II," *1st International Conference on Multi-Criterion Optimization*. 226-240. Zurich, Switzerland. 2001.

VITA

1st Lieutenant Mark R. Knarr was born and raised in Ft. Thomas, KY. He graduated from Highlands High School in 1994 and proceeded to the University of Cincinnati with an Air Force Reserve Officer Training Corps (AFROTC) scholarship. In June 1999 he received his officer's commission and graduated Suma Cum Laude with a Bachelor of Science degree in Civil & Environmental Engineering. He performed assignments at Eielson AFB, AK, and Columbus AFB, MS, and he entered the Graduate Engineering and Environmental Management program of the Graduate School of Engineering and Management, Air Force Institute of Technology, in August 2001.

REPORT DOCUMENTATION PAGE

Form Approved
OMB No. 074-0188

1. REPORT DATE *(DD-MM-YYYY)*	2. REPORT TYPE	3. DATES COVERED *(From – To)*
25-03-2003	**Master's Thesis**	Jun 2002 – Mar 2003

4. TITLE AND SUBTITLE

OPTIMIZING AN *IN SITU* BIOREMEDIATION TECHNOLOGY TO MANAGE PERCHLORATE-CONTAMINATED GROUNDWATER

5a. CONTRACT NUMBER

5b. GRANT NUMBER

5c. PROGRAM ELEMENT NUMBER

6. AUTHOR(S)

Knarr, Mark, R., Lieutenant, USAF

5d. PROJECT NUMBER
ENR #02-268

5e. TASK NUMBER

5f. WORK UNIT NUMBER

7. PERFORMING ORGANIZATION NAMES(S) AND ADDRESS(S)
Air Force Institute of Technology
Graduate School of Engineering and Management (AFIT/EN)
2950 P Street, Building 640
WPAFB OH 45433-7765

8. PERFORMING ORGANIZATION REPORT NUMBER

AFIT/GEE/ENV/03-14

9. SPONSORING/MONITORING AGENCY NAME(S) AND ADDRESS(ES)

AFCEE/ERT 210-536-4311
Attn: Ms. Erica Becvar
3207 North Rd., Bldg 532
Brooks AFB TX 78235-5363

ESTCP Program Office 703-696-2118
Attn: Dr. Andrea Leeson
901 N Stuart St., Ste 303
Arlington VA 22203

10. SPONSOR/MONITOR'S ACRONYM(S)

11. SPONSOR/MONITOR'S REPORT NUMBER(S)

12. DISTRIBUTION/AVAILABILITY STATEMENT

APPROVED FOR PUBLIC RELEASE; DISTRIBUTION UNLIMITED.

13. SUPPLEMENTARY NOTES

14. ABSTRACT

An innovative technology that is under development uses recirculation wells to mix electron donor into perchlorate-contaminated groundwater, *in situ*, to stimulate indigenous bacteria to reduce the perchlorate to innocuous products. To implement the technology, project managers need to understand how site conditions and technology design parameters impact performance. One way to gain this understanding is to use a technology model to optimize performance for given site conditions. In particular, a project manager will desire a system design that 1) maximizes perchlorate destruction, 2) minimizes treatment expense, and 3) attains regulatory limits on downgradient contaminant concentrations. Unfortunately, for a relatively complex technology with a number of engineering design parameters, as well as multiple objectives, system optimization is not straightforward.

In this study, a multi-objective genetic algorithm is used to determine design parameter values (such as water flow rate and well spacing) that maximize perchlorate destruction while minimizing cost. Optimization runs are conducted for differing site conditions. Results from the runs indicate that the relationship between perchlorate mass removal and operating cost is positively correlated and nonlinear. For equivalent operating times and costs, the optimized solutions show that, as expected, the technology achieves higher mass removals for the site having both higher hydraulic conductivity and higher initial source concentration. Results from the optimization runs show that increased perchlorate mass removal is not necessarily correlated with diminished downgradient perchlorate concentration, suggesting that it may be important to incorporate minimization of downgradient perchlorate concentration as an additional objective or constraint in the multi-objective optimization scheme.

15. SUBJECT TERMS

Recirculation wells, groundwater remediation, perchlorate, genetic algorithm, multiple objective optimization, bioremediation, modeling

16. SECURITY CLASSIFICATION OF:			17. LIMITATION OF ABSTRACT	18. NUMBER OF PAGES	19a. NAME OF RESPONSIBLE PERSON
a. REPORT	b. ABSTRACT	c. THIS PAGE			Professor Mark N. Goltz, ENV
U	U	U	UU	112	19b. TELEPHONE NUMBER *(Include area code)* (937) 255-3636, ext 4638; e-mail: Mark.Goltz @afit.edu